

A chemist, spectroscopist... discovering

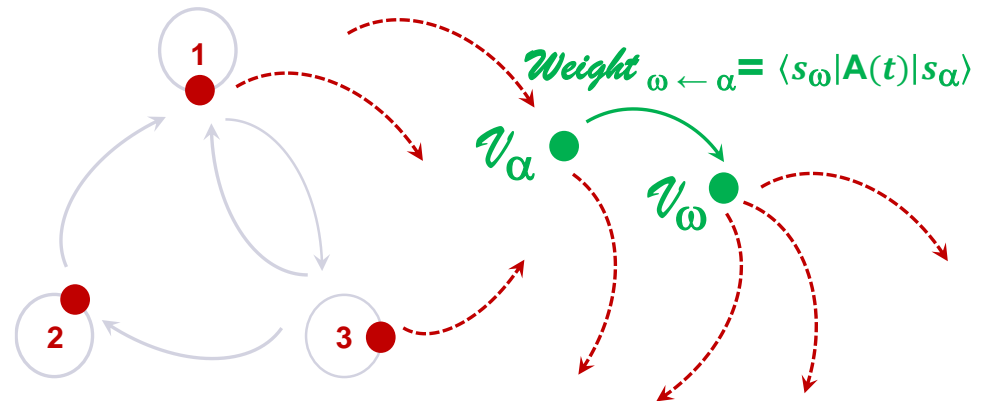
Path-Sum

C. Bonhomme¹, P.-L. Giscard²

¹ Laboratoire de Chimie de la Matière Condensée de Paris, Sorbonne Université, Paris, France

² Laboratoire Joseph Liouville, Université du Littoral Côte d'Opale, Calais, France

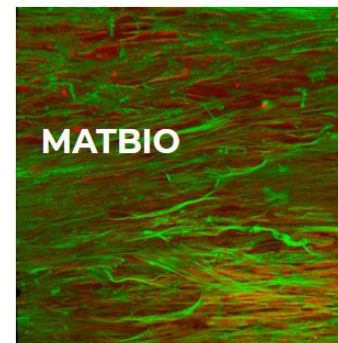
christian.bonhomme@upmc.fr

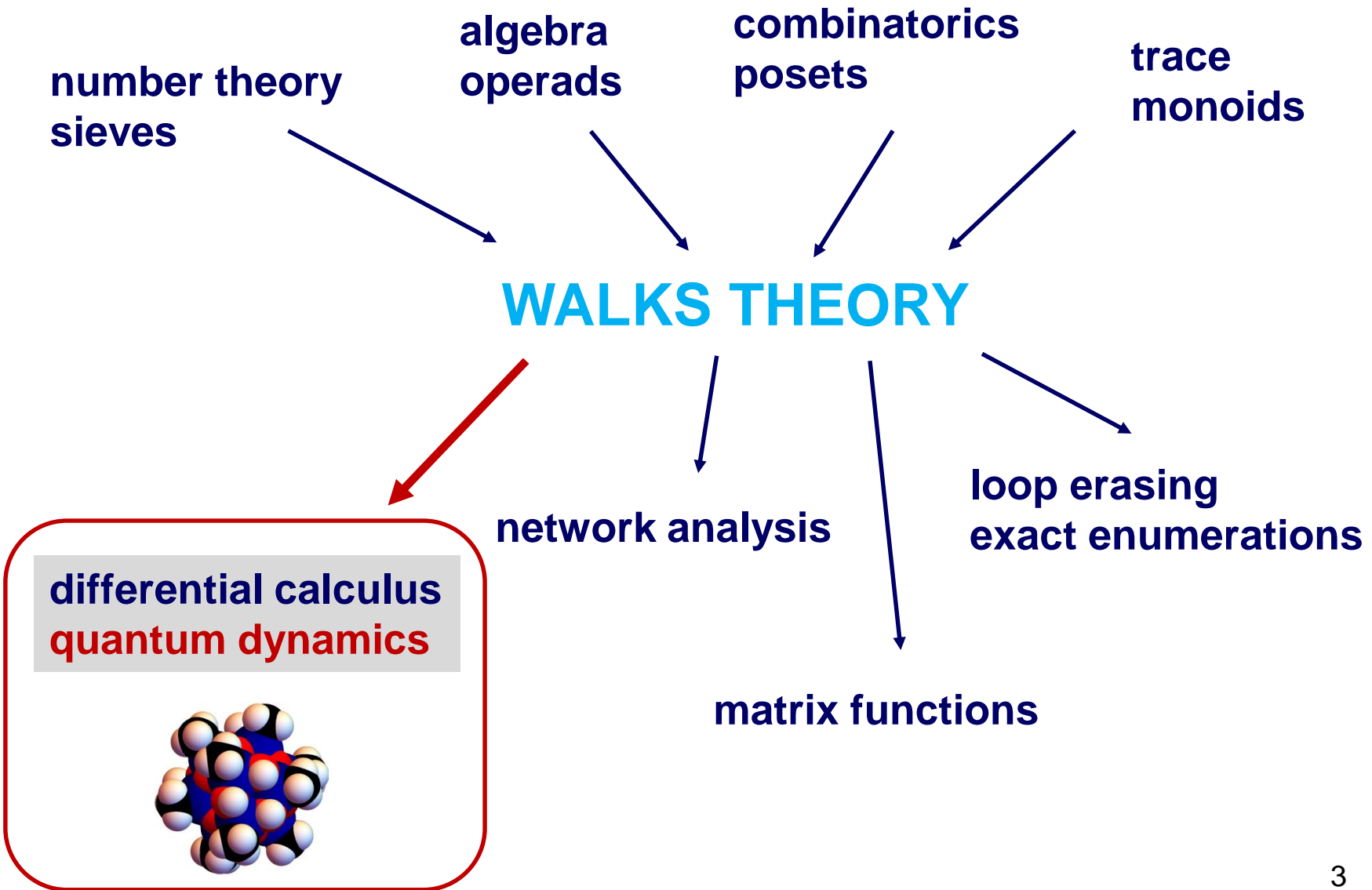


WACA workshop – Calais, France – May, 2021

LCMCP : <https://lcmcp.upmc.fr/site/>

Le laboratoire de Chimie de la Matière Condensée de Paris (UMR 7574 Sorbonne Université, CNRS, Collège de France) est un acteur reconnu dans le domaine de l'élaboration par des voies de chimie douce de matériaux fonctionnels inorganiques ou hybrides organiques-inorganiques, et sur l'évaluation de leurs propriétés physico-chimiques à différentes échelles.



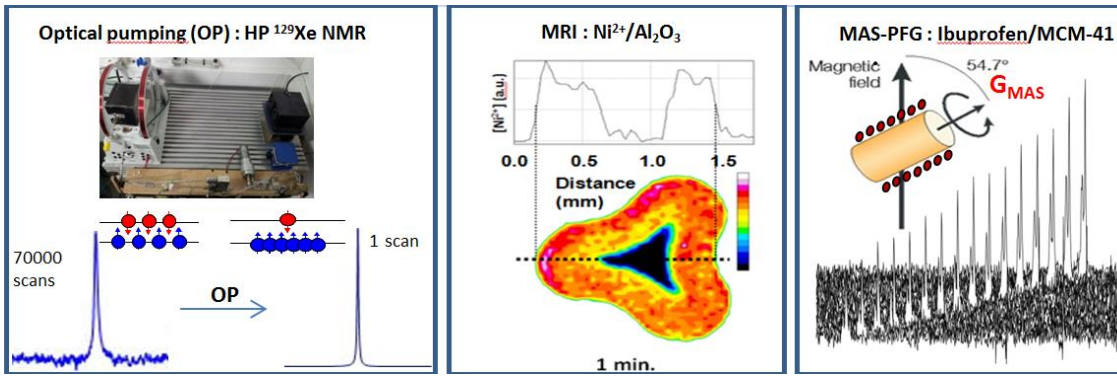


SMILES group @LCMCP

hyperpolarization
instrumentation

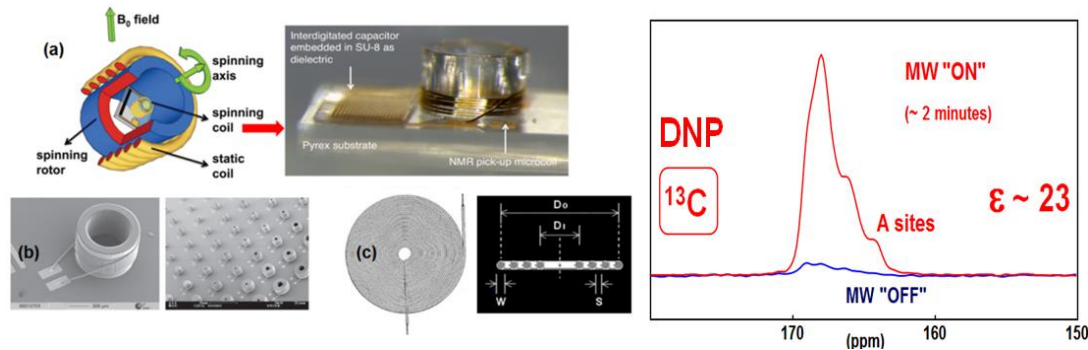
Diffusion by MAS-PFG NMR,
MRI, hyperpolarized ^{129}Xe
NMR : applications to porous
materials.

Coll.: IFFI, CN



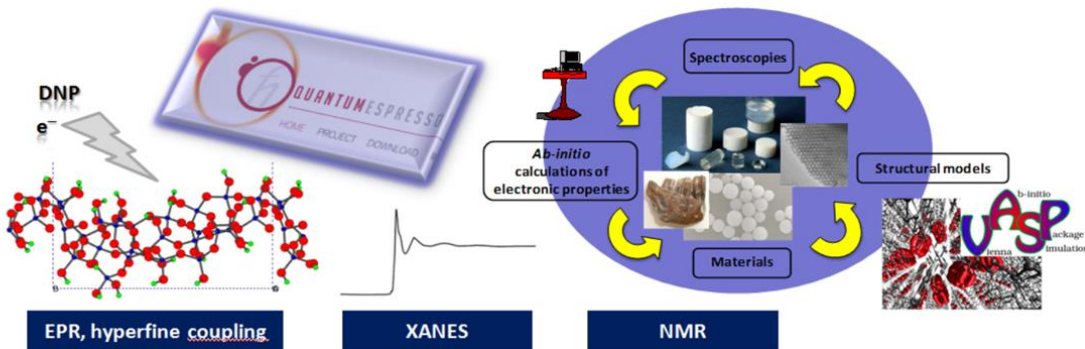
Instrumentation and
methodology in solid state
NMR: towards a net increase
in sensitivity!

Coll.: D. Sakellariou (CEA,
Saclay), V. Badilta
(Freiburg), F. Aussénac
(Bruker, Wissembourg).



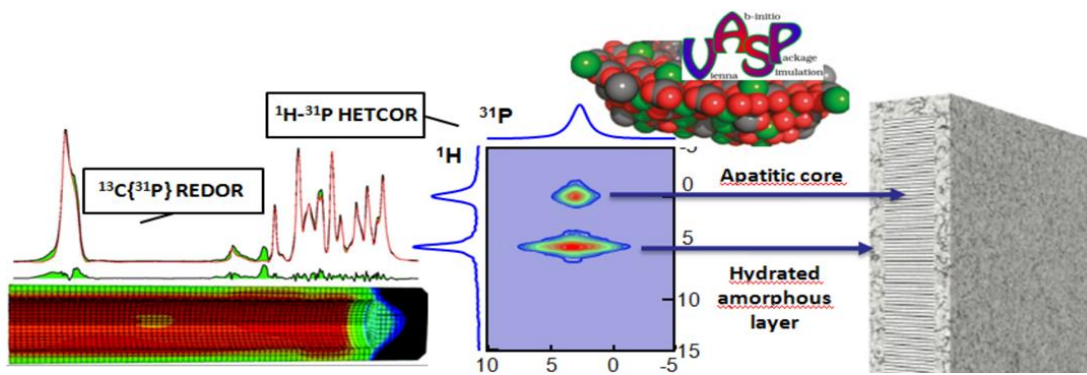
first-principles
calculations

The combined approach:
"advanced NMR / *ab initio*
calculations of NMR
parameters"; modeling of
hybrid interfaces.



biomineralization
pathological calcifications

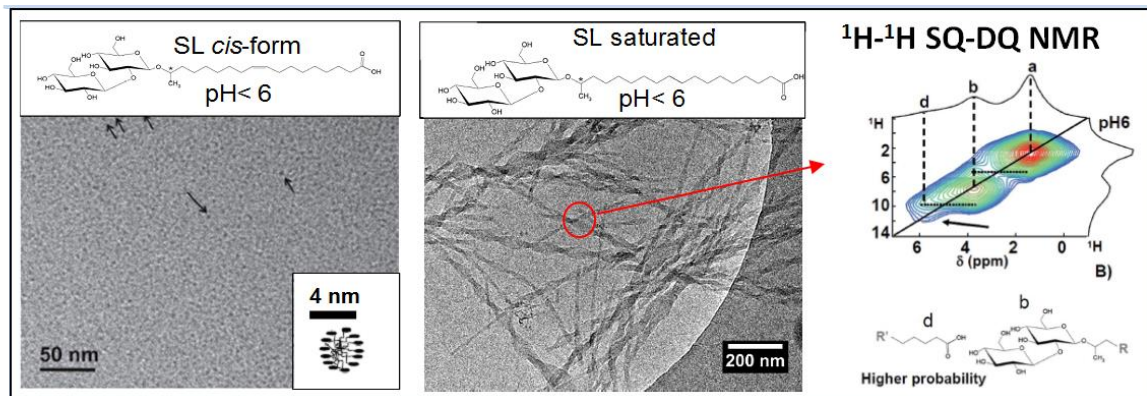
Two dimensional NMR and modeling new tools for the characterization of hybrid interfaces in biological materials (bones, teeth...).



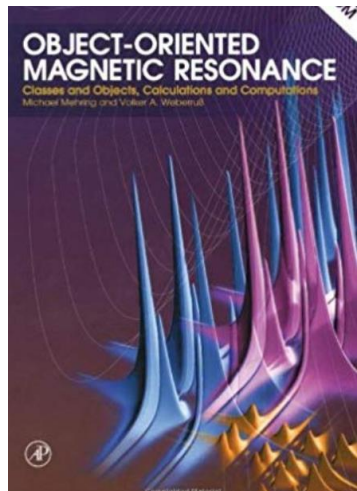
soft matter

Stimuli-responsive self-assembly of microbial glycolipids from biomass

Coll.: University of Gent, Belgium.



NMR, quantum mechanics and textbooks



■ Schrödinger equation

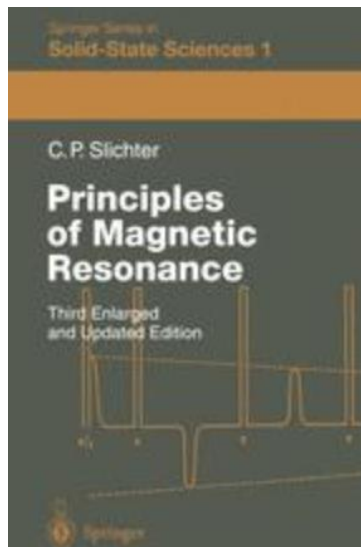
$$\frac{\partial}{\partial t} |\Psi(t)\rangle = -\frac{2\pi i}{\hbar} H(t) |\Psi(t)\rangle$$

state vector

■ Liouville – von Neumann equation

$$\frac{d}{dt} \rho(t) = -\frac{2\pi i}{\hbar} [H(t), \rho(t)]$$

density operator



U(t',t): the evolution operator

$$\rho(t') = U(t', t) \rho(t) U^*(t', t)$$

$$U(t', t) = \exp\left[\frac{2\pi i}{\hbar} H(t' - t)\right]$$

if H is time independent...

The evolution operator $U(t)$

Dyson time-ordering operator

$$U(t', t) = \text{OE}[-i H(t', t)] = T \exp(-i \int_t^{t'} H(\tau) d\tau)$$

$$U(\tau_c) = \exp\left(-i\tau_c \sum_{n=0}^{\infty} \overline{H^{(n)}}\right)$$

$$\bar{H} = {}^{(0)}\hat{H} - \frac{1}{2} \sum_{n \neq 0} \frac{\left[{}^{(-n)}\hat{H}, {}^{(n)}\hat{H} \right]}{n\omega_m} + \frac{1}{2} \sum_{n \neq 0} \frac{\left[\left[{}^{(n)}\hat{H}, {}^{(0)}\hat{H} \right], {}^{(-n)}\hat{H} \right]}{(n\omega_m)^2}$$

Magnus

Floquet

$$+ \frac{1}{3} \sum_{k,n \neq 0} \frac{\left[{}^{(n)}\hat{H}, \left[\hat{H}, {}^{(-n-k)}\hat{H} \right] \right]}{kn\omega_m^2} + \dots$$

G. Floquet, *Ann. Sci. Ecole Norm. Sup.*, 1883

F.J. Dyson, *Phys. Rev.*, 1949

W. Magnus, *Pure Appl. Math.*, 1954

F. Fer, *Bull. Classe Sci. Acad. Roy. Bel.*, 1958

J.H. Shirley, *Phys. Rev.*, 1965

U. Haeberlen, J.S. Waugh, *Phys. Rev.*, 1968

M.M. Maricq, *Phys. Rev.*, 1982

S. Vega, E.T. Olejniczak, R.G. Griffin, *J. Chem. Phys.*, 1984

I. Scholz, B.H. Meier, M. Ernst, *J. Chem. Phys.*, 2007

M. Leskes, P.K. Madhu, S. Vega, *Progress in NMR Spect.*, 2010

M. Goldman, P. J. Grandinetti, A. Llor *et al.*, *J. Chem. Phys.* 1992

E.S. Mananga, *Solid State NMR*, 2013

K. Takegoshi, N. Miyazawa, K. Sharma, P. K. Madhu, *J. Chem. Phys.*, 2015

...

The evolution operator $U(t)$

- general *mathematical* problem of coupled LDE with non-constant coefficients $a(t')$, $b(t')\dots$

$$A(t')U(t', t) = \frac{d}{dt'} U(t', t), \quad U(t, t) = \text{Id},$$

$$A(t') = \begin{pmatrix} a(t') & b(t') & \dots \\ c(t') & \dots & \dots \\ \dots & \dots & \dots \end{pmatrix}$$

N (finite)

N
bounded (over [t , t'])

↓ Dyson time-ordering operator (1952)

$$U(t', t) = \mathcal{T} \exp \left(\int_t^{t'} A(\tau) d\tau \right)$$

ordered exponential (OE)

↓ Floquet (1883) (if A periodic)

Magnus (1954)

perturbative treatment
convergence (?)

voudrions-nous développer indépendamment une approche nouvelle de l'opérateur d'évolution fondée sur l'approximation de Lie-Trotter-Suzuki : il s'agit tout simplement d'exprimer un opérateur exponentiel comme une limite à l'infini. De plus, il semble que l'approximation de Suzuki conduise naturellement à la description du système de spins par les chemins de Feynman. A notre connaissance, une telle description n'a pas encore été envisagée dans le cadre de la RMN.



De BONHOMME Christian★

Sujet A propos de votre article "An exact formulation..."

Pour pierre-louis.giscard@york.ac.uk★, BONHOMME Christian★

Bonjour Pierre-Louis,

mon nom est Christian Bonhomme et je suis Professeur de Chimie à l'UPMC, Paris.

Mon domaine de recherche est la RMN du solide, un domaine où l'expansion de Magnus fait référence.

J'ai été très impressionné par vos articles concernant la théorie des graphes et en particulier votre contribution : "An exact formulation of the time-ordered exponential using path-sums".

A mon sens, il s'agit d'un travail considérable qui devrait pouvoir être utilisé directement en RMN.

Aujourd'hui, j'essaie de m'initier à la théorie des graphes et à ses applications. J'aimerais être en particulier autonome pour effectuer des calculs tels que ceux présentés en exemples dans votre article (calculs des exp. ordonnées).

Vous serait-il possible de me guider de façon à ce que je sois plus efficace ? Seriez-vous d'accord pour engager une discussion ?

Très amicalement

Christian Bonhomme, Professeur à l'UPMC

An exact formulation of the time-ordered exponential using path-sums

Cite as: J. Math. Phys. 56, 053503 (2015); <https://doi.org/10.1063/1.4920925>

Submitted: 29 October 2014 . Accepted: 29 April 2015 . Published Online: 11 May 2015

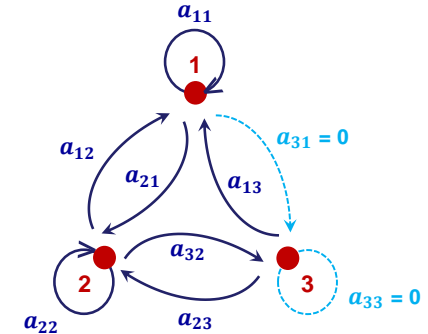
P.-L. Giscard, K. Lui, S. J. Thwaite, and D. Jaksch

Supprimer Autres ▾

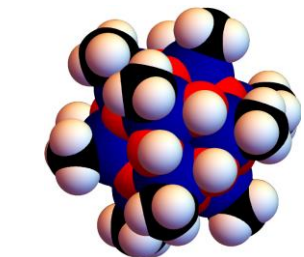
16/07/2017 à 19:17

Outline

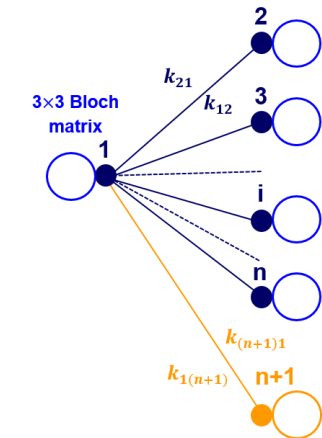
■ Basics of Path-Sum (Giscard)



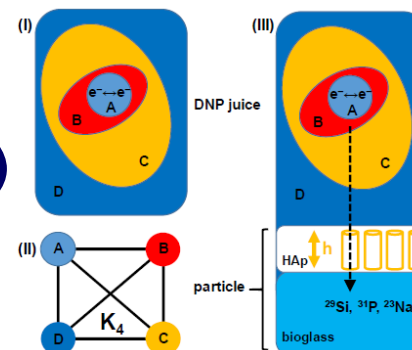
■ Bloch-Siegert effect and spin diffusion in solids



■ Bloch equations in MRI



■ the MAGICA project (2021 →)



The Path-Sum approach (P.-L. Giscard, 2015)

$$(f * g) = \int_t^{t'} f(t', \tau) g(\tau, t) d\tau$$

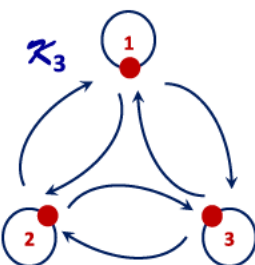
► Descending Ladder Principle (DLP)

(a)

$$H(t) = \begin{pmatrix} h_{11}(t) & h_{12}(t) & h_{13}(t) \\ h_{21}(t) & h_{22}(t) & h_{23}(t) \\ h_{31}(t) & h_{32}(t) & h_{33}(t) \end{pmatrix}$$

dynamical weighted graph (\mathcal{G})

(b)



(c)

$$U(t', t) = \begin{bmatrix} \int_t^{t'} G_{K_3,11}(\tau, t) d\tau & U_{12}(t', t) & U_{13}(t', t) \\ U_{21}(t', t) & \int_t^{t'} G_{K_3,22}(\tau, t) d\tau & U_{23}(t', t) \\ U_{31}(t', t) & U_{32}(t', t) & \int_t^{t'} G_{K_3,33}(\tau, t) d\tau \end{bmatrix}$$

each entry is given analytically

(d)

$$G_{K_3,11} = [1_* - h_{11} - h_{12} * G_{K_3 \setminus \{1\},22} * h_{21} - h_{13} * G_{K_3 \setminus \{1\},33} * h_{31}]^{*-1}$$

3 vertices

$$- h_{13} * G_{K_3 \setminus \{1\},33} * h_{32} * G_{K_3 \setminus \{1\},22} * h_{21}$$

$$- h_{12} * G_{K_3 \setminus \{1\},22} * h_{23} * G_{K_3 \setminus \{1\},33} * h_{31}]^{*-1}$$

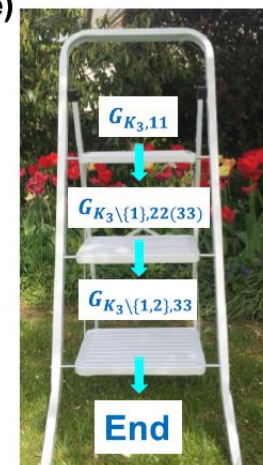
2 vertices

$$G_{K_3 \setminus \{1\},22} = [1_* - h_{22} - h_{23} * G_{K_3 \setminus \{1,2\},33} * h_{32}]^{*-1}$$

1 vertex

$$G_{K_3 \setminus \{1,2\},33} = [1_* - h_{33}]^{*-1}$$

(e)



infinite series of walks transformed into a single, finite, branched continued fraction

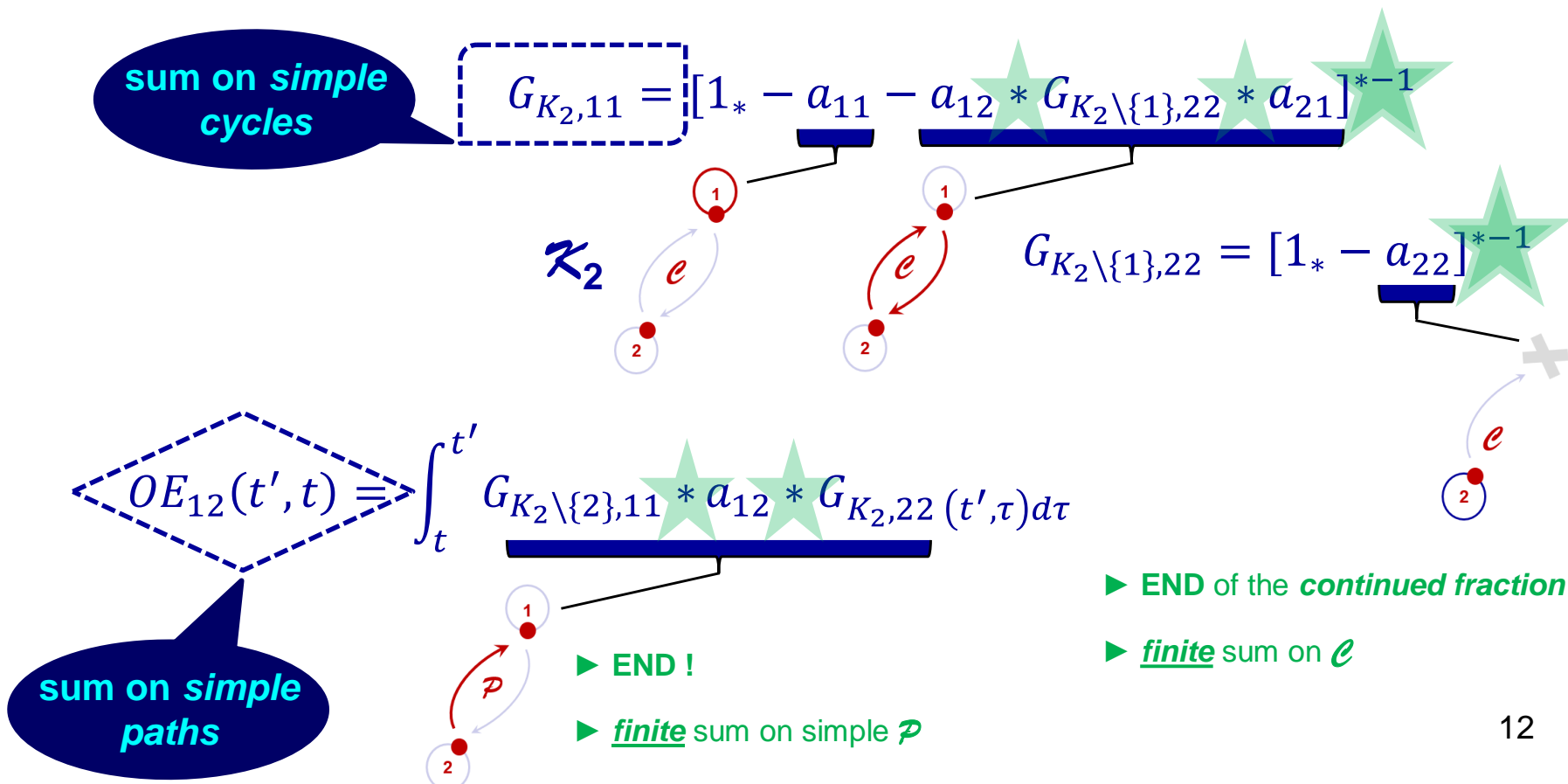
An example: 2×2 matrix

$$(f * g) = \int_t^{t'} f(t', \tau) g(\tau, t) d\tau$$

$$[1_* - (* \ * \ * \dots)]^{*-1} = \sum_{n \geq 0} (* \ * \ * \dots)^{*n}$$

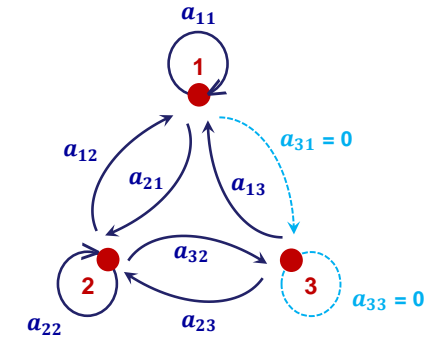
$$\text{OE}[A](t', t) = \begin{pmatrix} \int_t^{t'} G_{K_2,11}(t', \tau) d\tau \\ OE_{21}(t', t) \\ a_{ij}(t) \\ \int_t^{t'} G_{K_2,22}(t', \tau) d\tau \end{pmatrix}$$

Neumann series (analytical)
linear Volterra (2nd kind) (numerical)

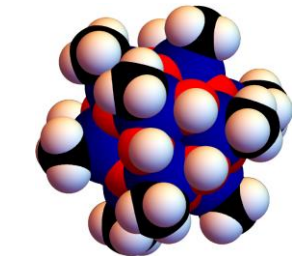


Outline

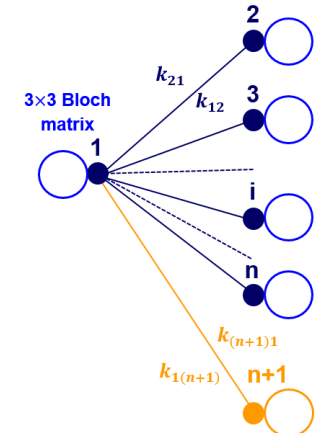
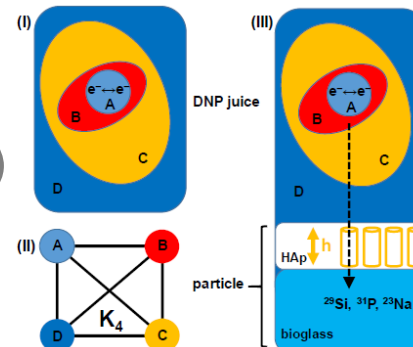
■ Basics of Path-Sum (Giscard)



■ Bloch-Siegert effect and spin diffusion in solids



■ Bloch equations in MRI



■ the MAGICA project (2021 →)

Circularly polarized excitation (test model)

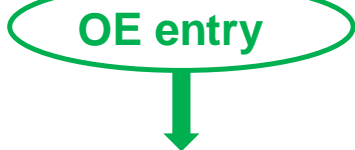
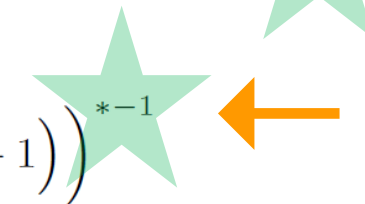
$$\mathbf{H}(t) = \frac{1}{2} \omega_0 \sigma_z + \beta [\sigma_x \cos(\omega t) + \sigma_y \sin(\omega t)]$$

$$\mathbf{H}(t) = \begin{pmatrix} \frac{\omega_0}{2} & \beta e^{-i\omega t} \\ \beta e^{i\omega t} & -\frac{\omega_0}{2} \end{pmatrix}, [\mathbf{H}(t'), \mathbf{H}(t)] \neq 0$$

$[1_* - (* * * \dots)]^{*-1}$

Path-Sum

$$G_{K_2,11}(t) = \left(1_* - \frac{\omega_0}{2i} + \frac{i\beta^2}{\Delta} \left(e^{-i\Delta(t'-t)} - 1 \right) \right)^{*-1}$$



Neumann series

$$OE[-i\mathbf{H}](t)_{11} = 1 + \sum_{n=0}^{\infty} \frac{(-it\beta^2/\Delta)^{n+1}}{(n+1)!} \sum_{k=0}^{n+1} \binom{n+1}{k} \left(\frac{\Delta\omega_0}{2\beta^2} - 1 \right)^k {}_2F_1 \left(-k, -k+n+1; -n-1; \frac{\Delta^2}{\Delta\omega_0 - \beta^2} \right)$$

Gauss hypergeometric



OE $[-i\mathbf{H}](t)$

$$\begin{pmatrix} e^{-\frac{1}{2}it(\Delta + \frac{\omega_0}{2})} (\cos(\alpha t/2) + \frac{i}{\alpha} (\Delta - \frac{\omega_0}{2}) \sin(\alpha t/2)) & -\frac{2i\beta}{\alpha} e^{-\frac{1}{2}it(\Delta + \frac{\omega_0}{2})} \sin(\alpha t/2) \\ -\frac{2i\beta}{\alpha} e^{\frac{1}{2}it(\Delta + \frac{\omega_0}{2})} \sin(\alpha t/2) & e^{\frac{1}{2}it(\Delta + \frac{\omega_0}{2})} (\cos(\alpha t/2) - \frac{i}{\alpha} (\Delta - \frac{\omega_0}{2}) \sin(\alpha t/2)) \end{pmatrix}$$

$$\mathbf{U}(t) = \exp\left(-\frac{1}{2}i\omega t \sigma_z\right) \exp\left(-it\left(\frac{1}{2}(\omega_0 - \omega)\sigma_z + \beta\sigma_x\right)\right)$$

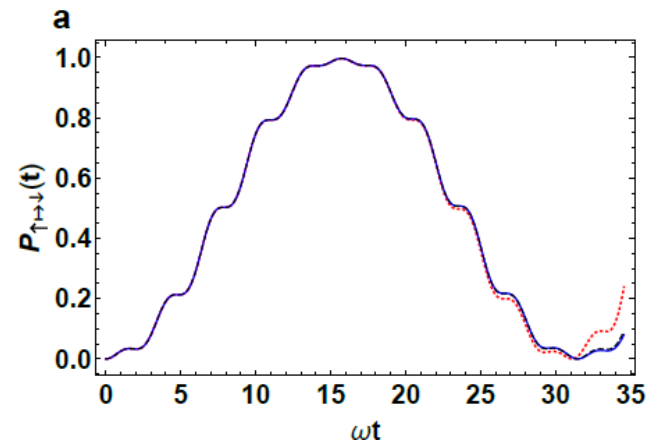
Linearly polarized excitation, Bloch-Siegert (BS) effect

$$\mathbf{H}(t) = \frac{1}{2} \omega_0 \boldsymbol{\sigma}_z + 2\beta \boldsymbol{\sigma}_x \cos(\omega t)$$

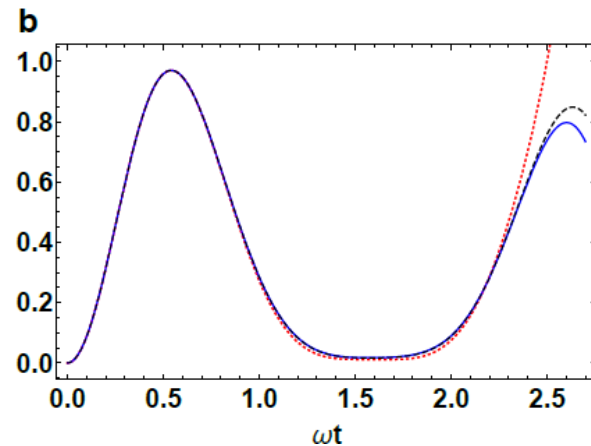
$$\mathbf{H}(t) = \begin{pmatrix} \frac{\omega_0}{2} & 2\beta \cos(\omega t) \\ 2\beta \cos(\omega t) & -\frac{\omega_0}{2} \end{pmatrix}$$

P(t) transition probability

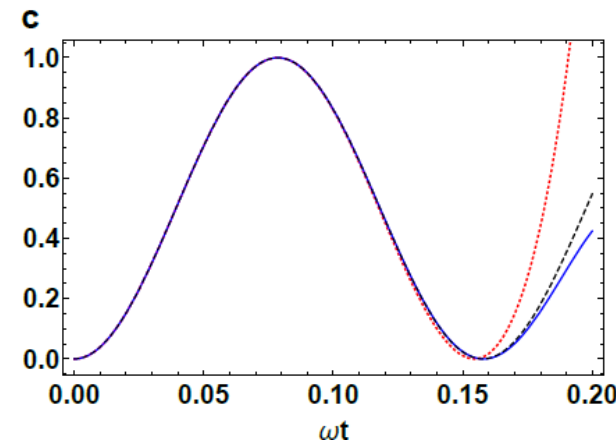
$\omega = \omega_0$ or $\omega \neq \omega_0$



$$\beta/\omega = 1/10$$



$$\beta/\omega = 3/2$$



$$\beta/\omega = 10$$

► analytical expression with few orders of the Neumann series

Linearly polarized excitation, Bloch-Siegert (BS) effect

PHYSICAL REVIEW RESEARCH 2, 023081 (2020)

Dynamics of quantum systems driven by time-varying Hamiltonians: Solution for the Bloch-Siegert Hamiltonian and applications to NMR

Pierre-Louis Giscard^{*}

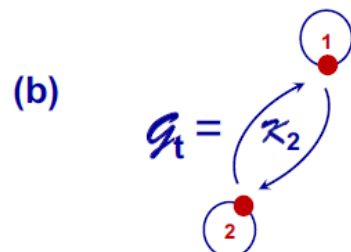
Université du Littoral Côte d'Opale, UR 2597, LMPA, Laboratoire de Mathématiques Pures et Appliquées Joseph Liouville,
F-62100 Calais, France

Christian Bonhomme[†]

Laboratoire de Chimie de la Matière Condensée de Paris, Sorbonne Université, UMR CNRS 7574,
4, place Jussieu, 75252, Paris Cedex 05, France

(Received 17 September 2019; accepted 30 March 2020; published 27 April 2020)

(a) $H(t) = \begin{pmatrix} h_{\uparrow}(t) & h_{\uparrow\downarrow}(t) \\ h_{\downarrow\uparrow}(t) & h_{\downarrow}(t) \end{pmatrix}$



(c) $U(t',t) = \begin{pmatrix} \int_t^{t'} G_{K_2,11}(\tau,t)d\tau & U_{\uparrow\uparrow}(t',t) \\ U_{\downarrow\uparrow}(t',t) & \int_t^{t'} G_{K_2,22}(\tau,t)d\tau \end{pmatrix}$

(d) $G_{K_2,11} = [1_* + i h_{\uparrow}] * G_{K_2 \setminus \{1\},22} * h_{\downarrow\uparrow}^{-1}$

2 vertices

1 vertex

$$G_{K_2 \setminus \{1\},22} = [1_* + i h_{\downarrow}]^{-1}$$

2 vertices

$$U_{\uparrow\uparrow}(t',t) = \int_t^{t'} G_{K_2 \setminus \{2\},11} * h_{\uparrow\uparrow} * G_{K_2,22}(\tau,t)d\tau$$

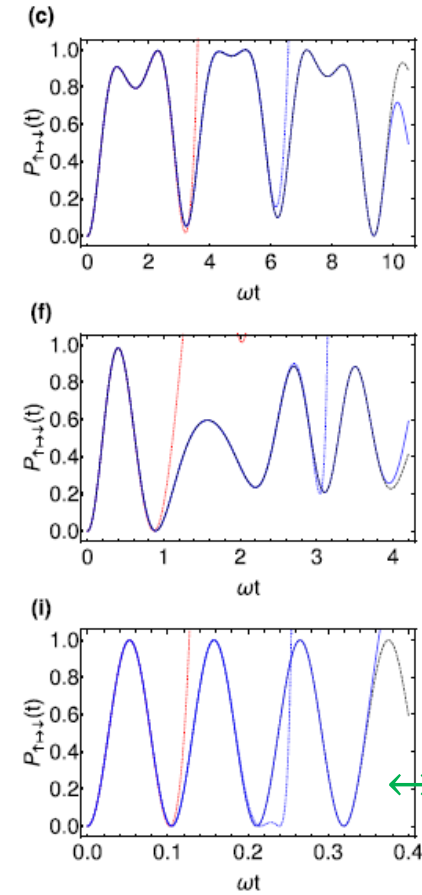
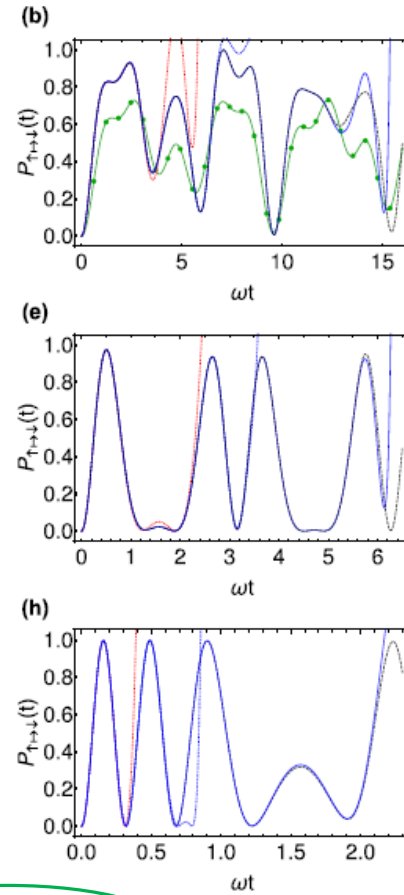
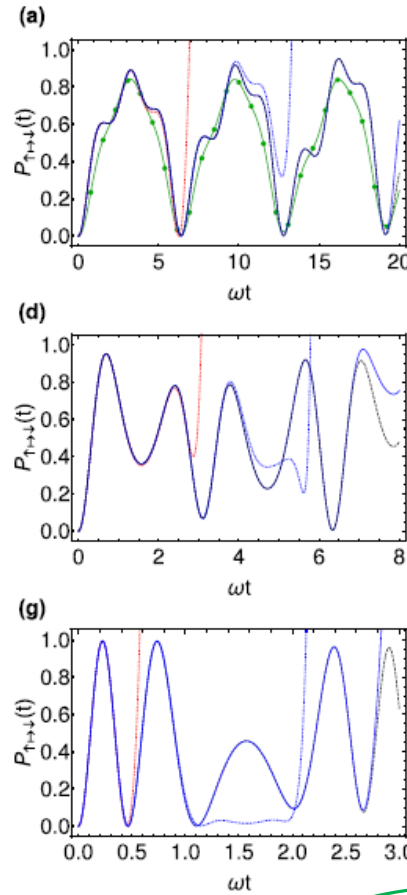
(e)



Linearly polarized excitation, Bloch-Siegert (BS) effect

Visualizing the solution

$$\downarrow \beta/\omega = 0.5$$



$$H(t) = \begin{pmatrix} \frac{\omega_0}{2} & 2\beta\cos(\omega t) \\ 2\beta\cos(\omega t) & -\frac{\omega_0}{2} \end{pmatrix}$$

$$\leftrightarrow \beta/\omega = 15$$

FIG. 3. Bloch-Siegert dynamics: resonant $\omega_0 = \omega$ transition probability $P_{\uparrow\rightarrow\downarrow}(t)$ as a function of time in the weak- to ultrastrong-coupling regimes, with (a) $\beta/\omega = 0.5$, (b) $\beta/\omega = 0.7$, (c) $\beta/\omega = 0.9$, (d) $\beta/\omega = 1.2$, (e) $\beta/\omega = 1.6$, (f) $\beta/\omega = 2$, (g) $\beta/\omega = 3.5$, (h) $\beta/\omega = 5$, and (i) $\beta/\omega = 15$. Shown here are the numerical solution (dashed black line) and the fully analytical formulas for the Neumann expansions of the exact path-sum solution $P_{\uparrow\rightarrow\downarrow}^{(3)}(t)$ (dotted red line), $P_{\uparrow\rightarrow\downarrow}^{(7)}(t)$ (dotted blue line), and $P_{\uparrow\rightarrow\downarrow}^{(13)}(t)$ (solid blue line) (see Appendix B). As seen here, each of these formulas are equally valid throughout the coupling regimes, from weak to ultrastrong. Whenever longer times are desired, higher orders of the path-sum solution are readily available *analytically*. Also shown in (a) and (b) are the second-order Floquet theory [11] (solid green line and green points). The Floquet result is not shown in subsequent figures, where it is wildly inaccurate. Parameters: two-level system driven by the Bloch-Siegert Hamiltonian of Eq. (8) [11,12] starting in the $|\uparrow\rangle$ state at $t = 0$.

Linearly polarized excitation, Bloch-Siegert (BS) effect

Visualizing the solution

$$\mathbf{H}(t) = \begin{pmatrix} \frac{\omega_0}{2} & 2\beta\cos(\omega t) \\ 2\beta\cos(\omega t) & -\frac{\omega_0}{2} \end{pmatrix}$$

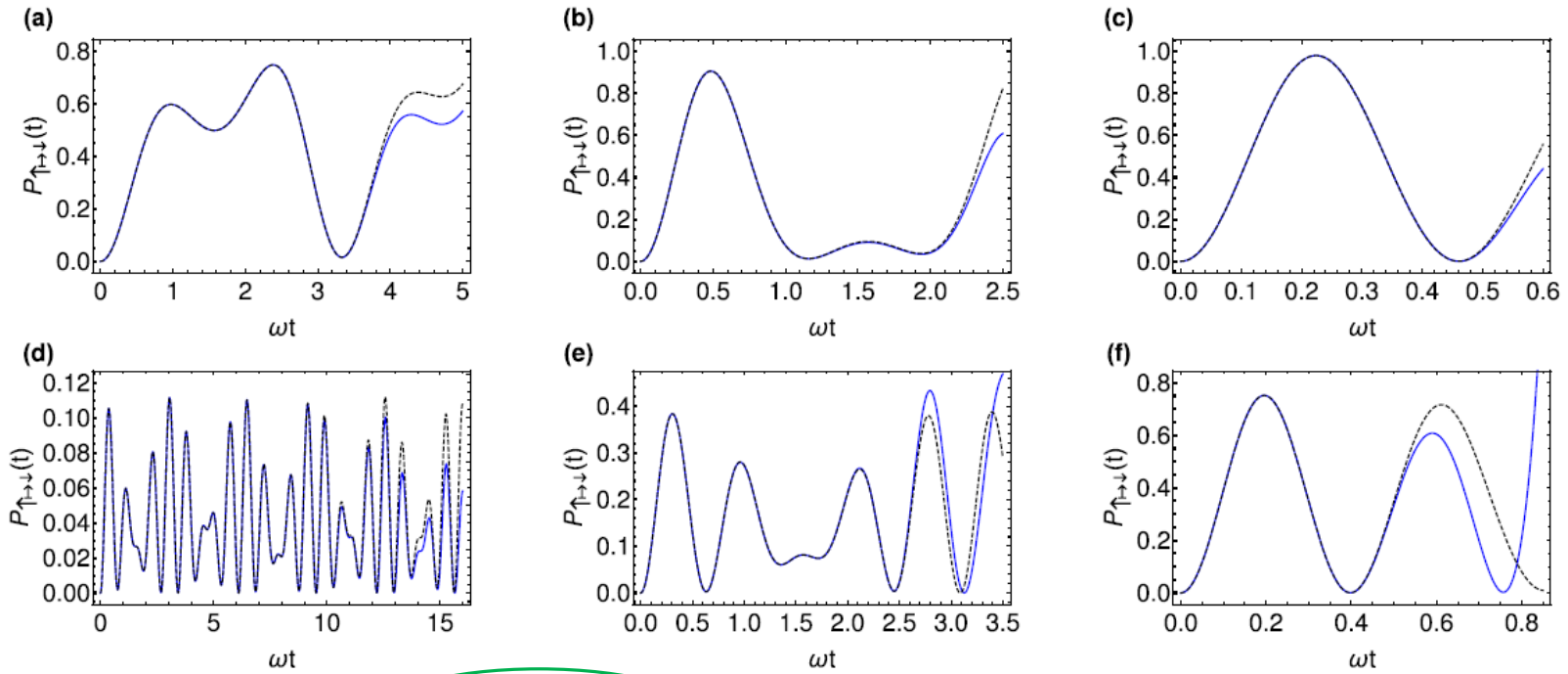
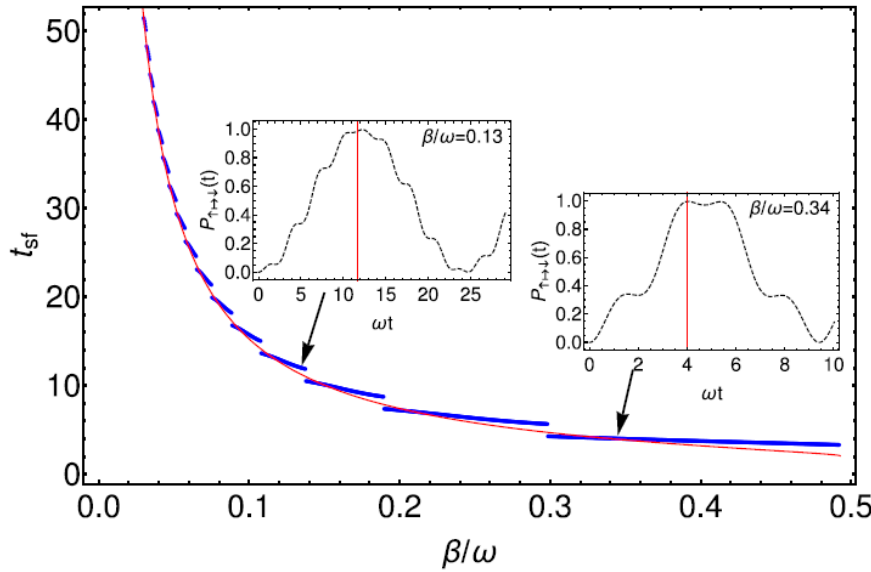


FIG. 4. Bloch-Siegert dynamics: off-resonance $\omega_0 \neq \omega$ transition probability $P_{\uparrow\downarrow}(t)$ as a function of time in the weak- to strong-coupling regimes, with (a) $\omega_0 = 2\omega$, $\beta/\omega = 0.7$, (b) $\omega_0 = 2\omega$, $\beta/\omega = 1.6$, (c) $\omega_0 = 2\omega$, $\beta/\omega = 3.5$, (d) $\omega_0 = 8\omega$, $\beta/\omega = 0.7$, (e) $\omega_0 = 8\omega$, $\beta/\omega = 1.6$, and (f) $\omega_0 = 8\omega$, $\beta/\omega = 3.5$. Shown here are the numerical solution (dashed black line) and the fully analytical formula for the Neumann expansion of the exact path-sum solution at the fourth order $P_{\uparrow\downarrow}^{(4)}(t)$ (solid blue line). Parameters: two-level system driven by the Bloch-Siegert Hamiltonian of Eq. (8) [11,12] starting in the $|\uparrow\rangle$ state at $t = 0$.

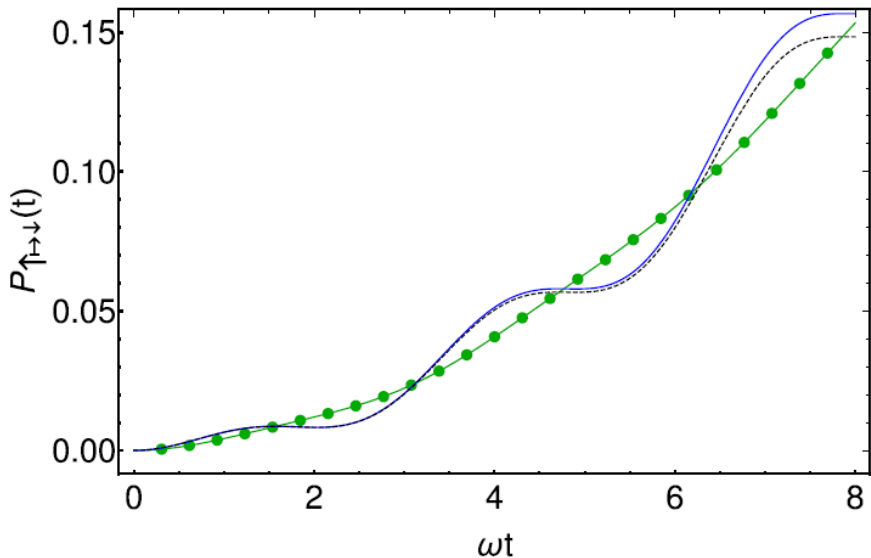
Linearly polarized excitation, Bloch-Siegert (BS) effect

Physical insights



$$\mathbf{H}(t) = \begin{pmatrix} \frac{\omega_0}{2} & 2\beta\cos(\omega t) \\ 2\beta\cos(\omega t) & -\frac{\omega_0}{2} \end{pmatrix}$$

$$\begin{aligned} t_{sf} &= \frac{1}{2\sqrt{2}} \sqrt{\frac{12}{\beta^2} - \frac{15}{\omega^2} + \frac{\sqrt{3}}{\beta^4\omega^2} \sqrt{91\beta^8 - 88\beta^6\omega^2 + 16\beta^4\omega^4}} \\ &= \frac{1}{\beta} \sqrt{\frac{1}{2}(3 + \sqrt{3})} - \frac{\beta}{8\omega^2} \sqrt{\frac{1}{2}(129 + 67\sqrt{3})} \\ &\quad - \frac{\beta^3}{128\omega^4} \sqrt{\frac{1}{2}(16131 + 5545\sqrt{3})} + O(\beta^4). \end{aligned} \quad (11)$$



Accelarated Neumann series

in the case of ultra-strong regime, i.e. $\beta/\omega_0 \gg 1$, then: $K_1(t) \gg K_2(t)$

$$K_1(t) = -2i\beta \begin{pmatrix} 0 & \cos(\omega t) \\ \cos(\omega t) & 0 \end{pmatrix}$$

$$K_2(t) = -i\omega_0 \begin{pmatrix} 1/2 & 0 \\ 0 & -1/2 \end{pmatrix}.$$

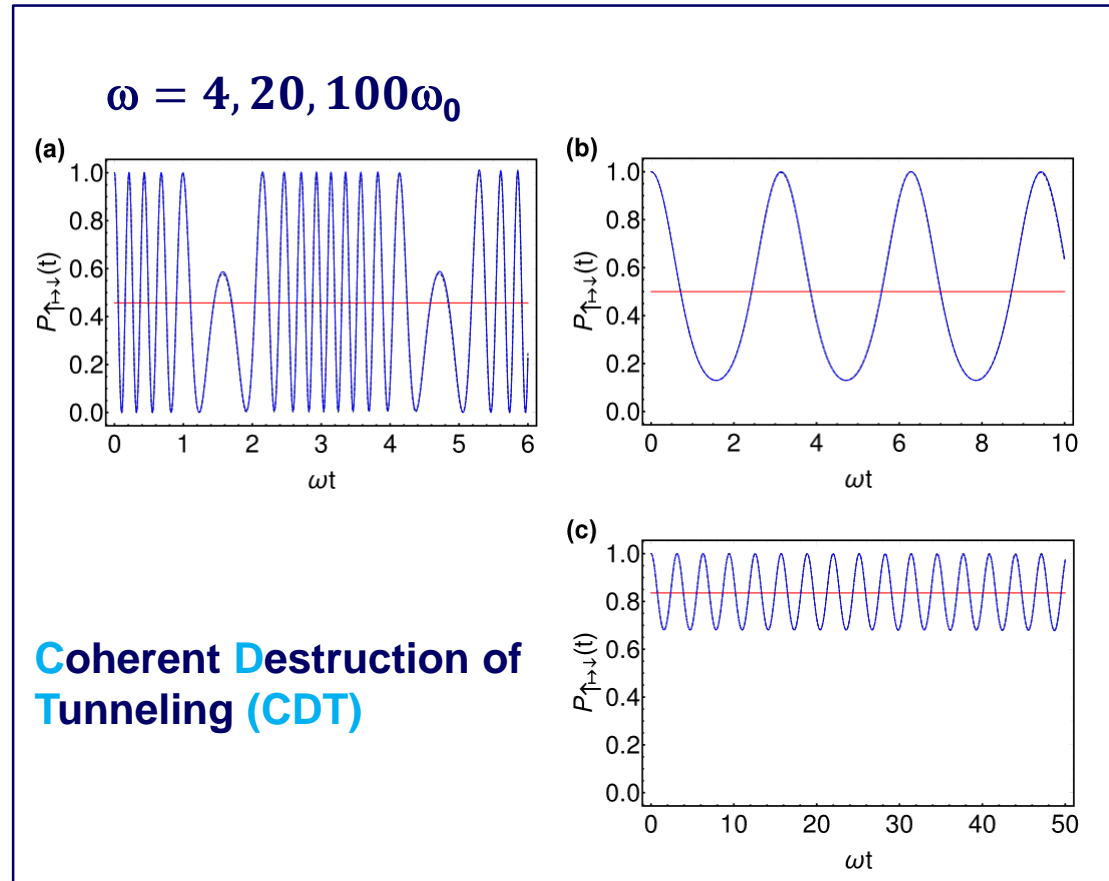
$$G^{(acc,0)}(t', t) = [U^{(acc,0)}(t', t)]'$$

$$= \int_t^{t'} G_1(t', \tau) G_2(\tau, t) d\tau.$$


related to individual K_i



the first term of the
accelerated analytical
Neumann series is
sufficient



Linearly polarized excitation, Bloch-Siegert (BS) effect

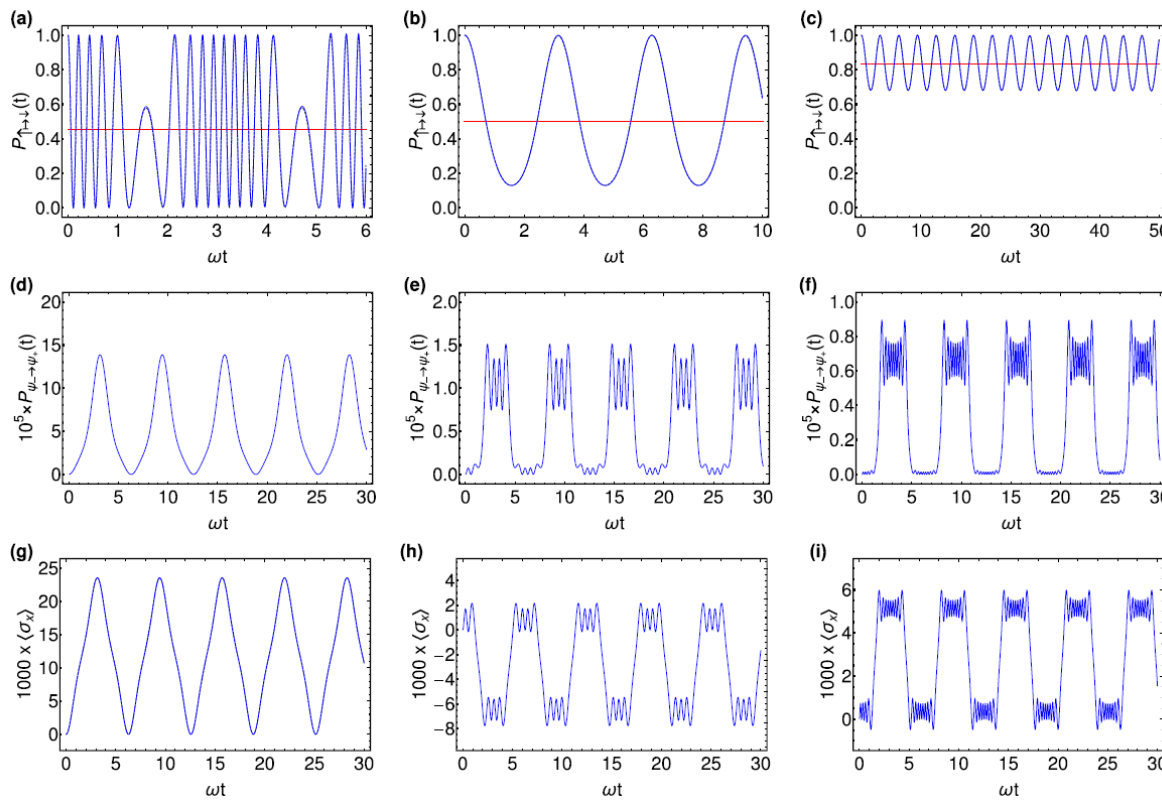
accelerated Neumann series $\rightarrow \beta / \omega_0 \gg 1$

(Giscard, 2020)

$$\mathbf{H}(t) = \begin{pmatrix} \frac{\omega_0}{2} & 2\beta \cos(\omega t) \\ 2\beta \cos(\omega t) & -\frac{\omega_0}{2} \end{pmatrix}$$



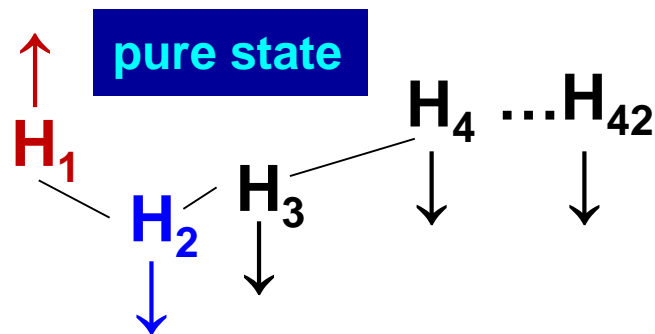
$$\mathbf{U}^{(acc,0)}(t) = \begin{pmatrix} \cos\left(\frac{2\beta}{\omega} \sin(\omega t)\right) + e^{-\frac{1}{2}i\omega_0 t} - 1 & -i \sin\left(\frac{2\beta}{\omega} \sin(\omega t)\right) \\ -i \sin\left(\frac{2\beta}{\omega} \sin(\omega t)\right) & \cos\left(\frac{2\beta}{\omega} \sin(\omega t)\right) + e^{\frac{1}{2}i\omega_0 t} - 1 \end{pmatrix} \\ + \int_0^t \begin{pmatrix} i\omega_0 e^{-\frac{1}{2}i\omega_0 \tau} \sin^2\left(\frac{2\beta}{\omega} [\sin(\omega \tau) - \sin(\omega t)]\right) & -\frac{1}{2}\omega_0 e^{\frac{1}{2}i\omega_0 \tau} \sin\left(\frac{4\beta}{\omega} [\sin(\omega \tau) - \sin(\omega t)]\right) \\ \frac{1}{2}\omega_0 e^{-\frac{1}{2}i\omega_0 \tau} \sin\left(\frac{4\beta}{\omega} [\sin(\omega \tau) - \sin(\omega t)]\right) & -i\omega_0 e^{\frac{1}{2}i\omega_0 \tau} \sin^2\left(\frac{2\beta}{\omega} [\sin(\omega \tau) - \sin(\omega t)]\right) \end{pmatrix} d\tau.$$



$$\sin[\alpha + z \sin(\phi)] = \sin(\alpha) \left(J_0(z) + 2 \sum_{n=0}^{\infty} J_{2n}(z) \cos(2n\phi) \right) + 2 \cos(\alpha) \sum_{n=0}^{\infty} J_{2m+1}(z) \sin[(2n+1)\phi]$$

Spin diffusion: N spin systems, homonuclear dipolar Hamiltonian, H_D

$t = 0$



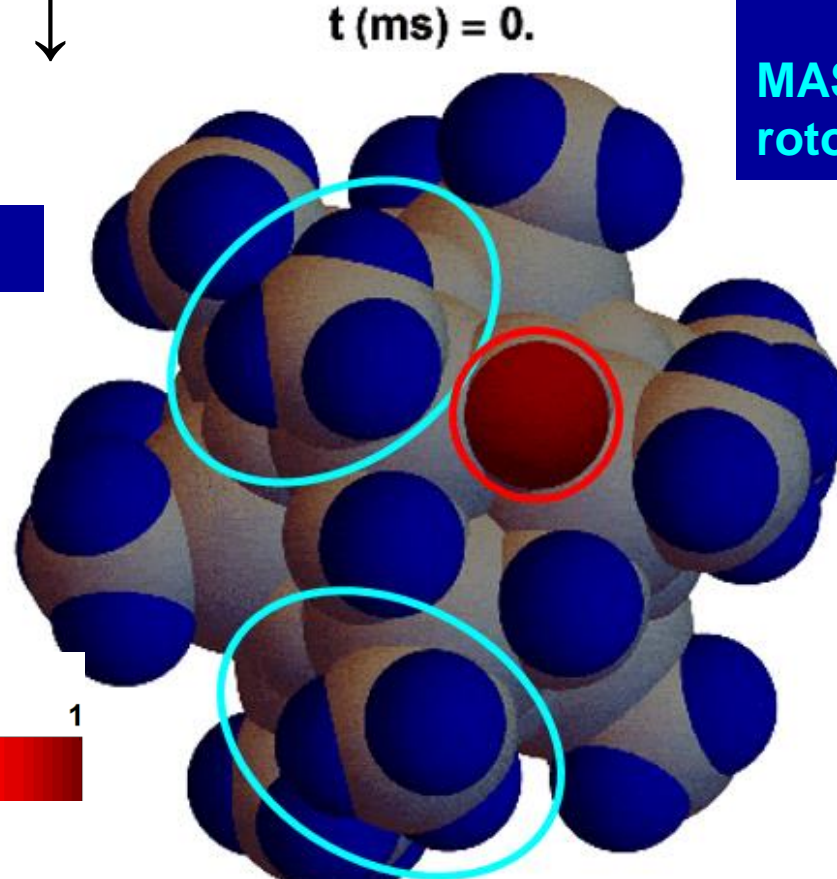
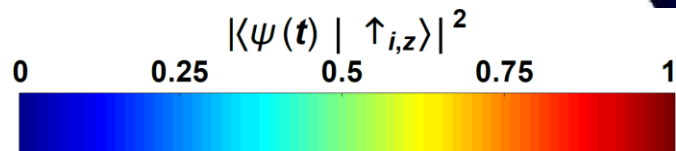
Coll.: F. Ribot, France

$(\text{CH}_3)_{12}(\text{OH})_6\text{Sn}_{12}$

42 protons
« rigid » CH_3

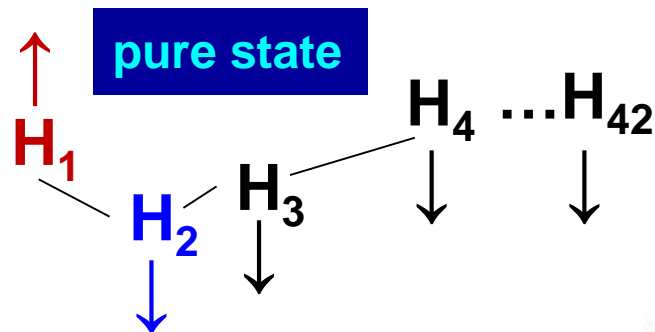
MAS 10 kHz
rotor period 0.1 ms

analytical expression



Spin diffusion: N spin systems, homonuclear dipolar Hamiltonian, H_D

$t = 0$



Coll.: F. Ribot, France

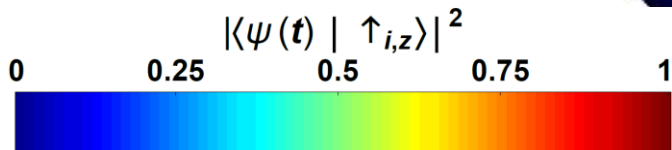
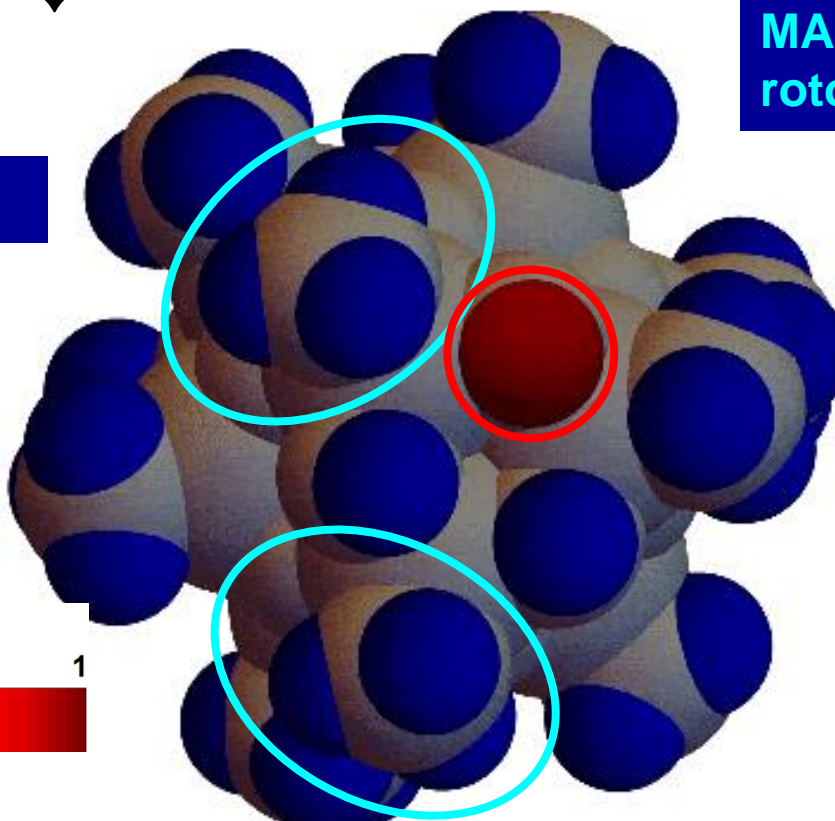
analytical expression



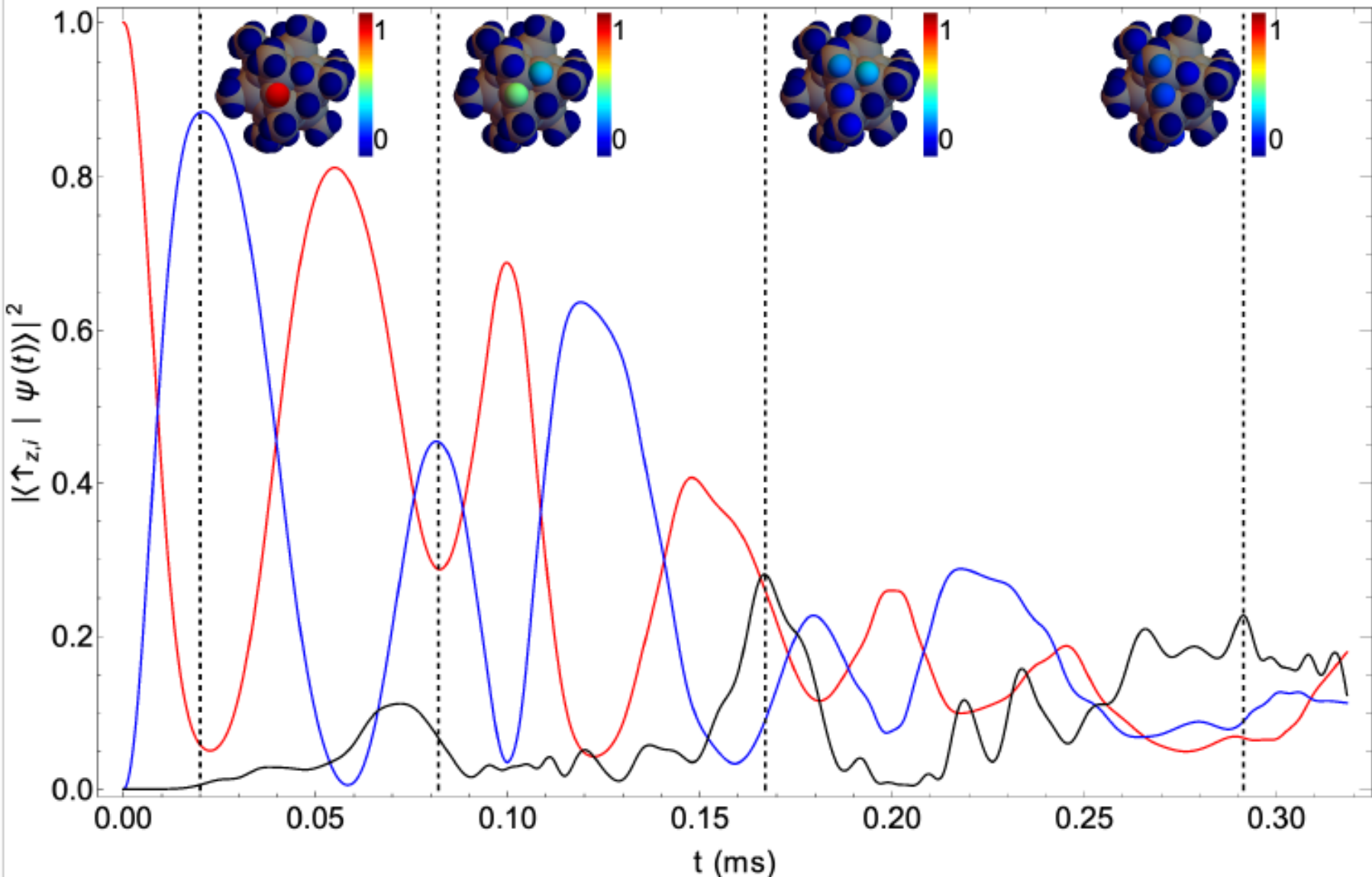
42 protons
« rigid » CH_3

MAS 10 kHz
rotor period 0.1 ms

$t (\text{ms}) = 0.$



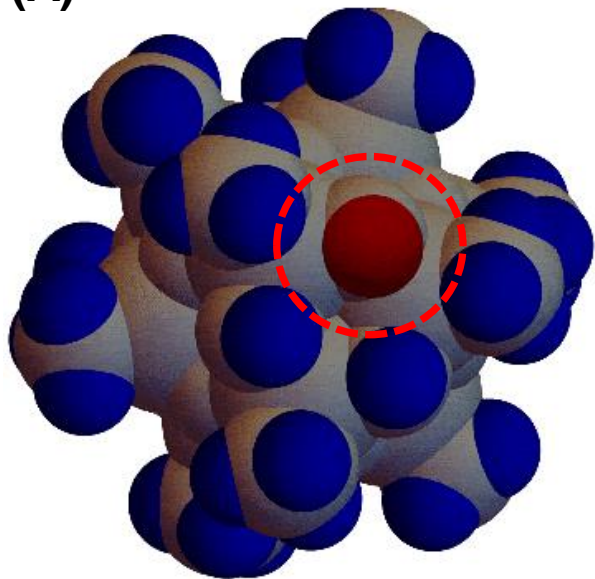
Spin diffusion: N spin systems, homonuclear dipolar Hamiltonian, H_D



Scale invariance of Path-Sum

► Path-Sum is used herein conjunction with all *state-space reduction* techniques

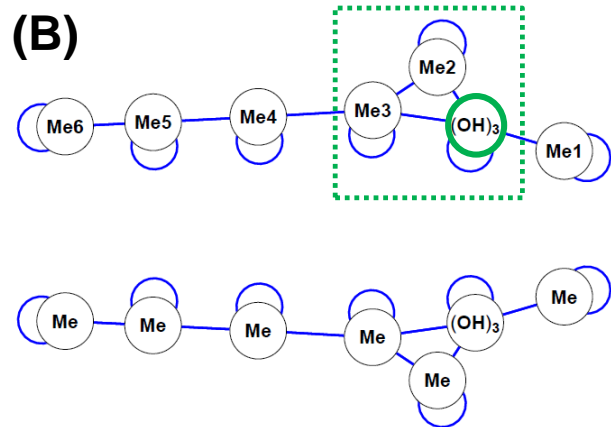
(A) $t \text{ (ms)} = 0.$



$(\text{CH}_3)_{12}(\text{OH})_6\text{Sn}_{12}$
42 protons
MAS 10 kHz
pure state

PARTITIONS

(B)



(C)



$$\begin{aligned} U_{(\text{OH})_3} = & 1 * \left(\text{Id}_* + iH_{(\text{OH})_3} + H_{(\text{OH})_3\text{Me}_1} * \Gamma_1 * H_{\text{Me}_1(\text{OH})_3} \right. \\ & + H_{(\text{OH})_3\text{Me}_2} * \Sigma_2 * H_{\text{Me}_2(\text{OH})_3} + H_{(\text{OH})_3\text{Me}_3} * \Sigma_3 * H_{\text{Me}_3(\text{OH})_3} \\ & - iH_{(\text{OH})_3\text{Me}_2} * \Gamma_2 * H_{\text{Me}_2\text{Me}_3} * \Sigma_3 * H_{\text{Me}_3(\text{OH})_3} \\ & \left. - iH_{(\text{OH})_3\text{Me}_3} * \Sigma_3 * H_{\text{Me}_3\text{Me}_2} * \Sigma_2 * H_{\text{Me}_2(\text{OH})_3} \right)^{-1}, \end{aligned}$$

$$\Sigma_2 = \frac{1}{\text{Id}_* + iH_{\text{Me}_2} + H_{\text{Me}_2\text{Me}_3} * \Sigma_3 * H_{\text{Me}_3\text{Me}_2}},$$

$$\Sigma_3 = \frac{1}{\text{Id}_* + iH_{\text{Me}_3} + H_{\text{Me}_3\text{Me}_4} * \Sigma_4 * H_{\text{Me}_4\text{Me}_3}},$$

$$\Sigma_4 = \frac{1}{\text{Id}_* + iH_{\text{Me}_4} + H_{\text{Me}_4\text{Me}_5} * \Sigma_5 * H_{\text{Me}_5\text{Me}_4}},$$

$$\Sigma_5 = \frac{1}{\text{Id}_* + iH_{\text{Me}_5} + H_{\text{Me}_5\text{Me}_6} * \Gamma_6 * H_{\text{Me}_6\text{Me}_5}},$$

Comments on the Path-Sum solution

the Path-Sum solution is:

$$G_{K_3,11} = [1_* - h_{11} - h_{12} * G_{K_3 \setminus \{1\},22} * h_{21} - h_{13} * G_{K_3 \setminus \{1\},33} * h_{31}]^{*-1}$$

$$- h_{13} * G_{K_3 \setminus \{1\},33} * h_{32} * G_{K_3 \setminus \{1\},22} * h_{21}$$

$$- h_{12} * G_{K_3 \setminus \{1\},22} * h_{23} * G_{K_3 \setminus \{1\},33} * h_{31}]^{*-1}$$

★

$$G_{K_3 \setminus \{1\},22} = [1_* - h_{22} - h_{23} * G_{K_3 \setminus \{1,2\},33} * h_{32}]^{*-1}$$

★

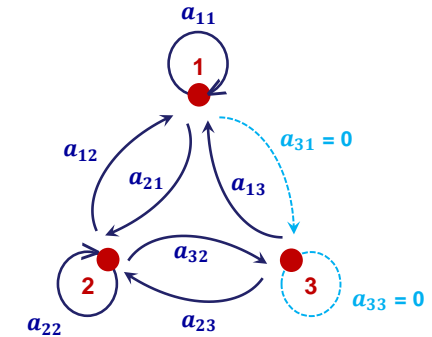
$$G_{K_3 \setminus \{1,2\},33} = [1_* - h_{33}]^{*-1}$$

★

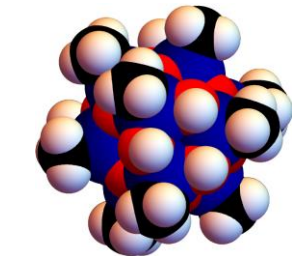
- ▶ **exact** as it captures the entire physics and mathematics of the problem as opposed to methods that are approximate, perturbative etc
 - ▶ **non perturbative, super exponentially CV**
 - ▶ **always closed form in**
- $[1_* - (* * * \dots)]^{*-1}$
- ▶ **Neumann series: analytic, closed form at fixed accuracy**
 - ▶ **Numerically at all orders: >> Zassenhaus**

Outline

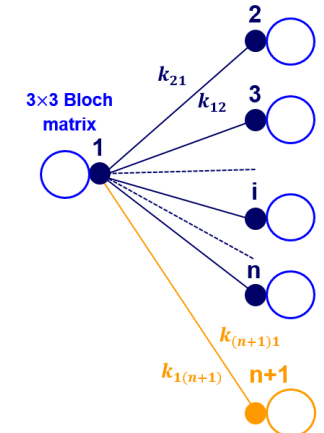
■ Basics of Path-Sum (Giscard)



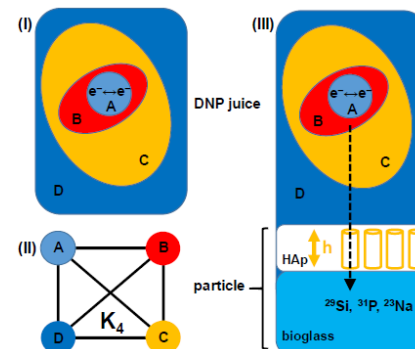
■ Bloch-Siegert effect and spin diffusion in solids



■ Bloch equations in MRI



■ the MAGICA project (2021 →)

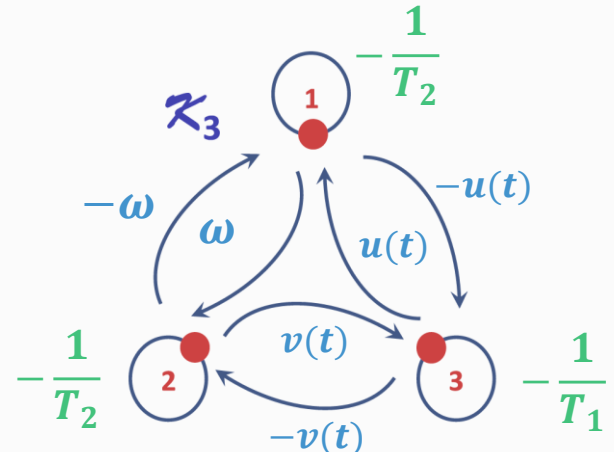


Bloch equations in the Path-Sum context

$$\frac{d}{dt} M(t) = \begin{pmatrix} -\frac{1}{T_2} & -\omega & u(t) \\ \omega & -\frac{1}{T_2} & -v(t) \\ -u(t) & v(t) & -\frac{1}{T_1} \end{pmatrix} M(t) + \begin{pmatrix} 0 \\ 0 \\ \frac{1}{T_1} M_0 \end{pmatrix}$$

RF fields, offset relaxation

U = OE [Φ] ? (very few solved examples)



relaxation → self-loops
 RF fields, offset → directed edges

Path-Sum

$$\Phi(t) = \begin{pmatrix} C_1 & \Phi_{12}(t) & \Phi_{13}(t) \\ \Phi_{21}(t) & C_2 & \Phi_{23}(t) \\ \Phi_{31}(t) & \Phi_{32}(t) & C_3 \end{pmatrix}$$

with: $C_1 \neq C_2 \neq C_3$, $\Phi_{13}(t) \neq -\Phi_{31}(t) \dots$

$$G = \frac{dU}{dt}$$

$$G_{11} = (1_* - C_1 - (\Phi_{12} + \Phi_{13} * \Phi_{32}) * G_{22 \setminus \{1\}} * \Phi_{21} - (\Phi_{13} + \Phi_{12} * \Phi_{23}) * G_{33 \setminus \{1\}} * \Phi_{31})^{*-1}$$

$$G_{22} = (1_* - C_2 - (\Phi_{21} + \Phi_{23} * \Phi_{31}) * G_{11 \setminus \{2\}} * \Phi_{12} - (\Phi_{23} + \Phi_{21} * \Phi_{13}) * G_{33 \setminus \{2\}} * \Phi_{32})^{*-1}$$

$$G_{33} = (1_* - C_3 - (\Phi_{32} + \Phi_{31} * \Phi_{12}) * G_{22 \setminus \{3\}} * \Phi_{23} - (\Phi_{31} + \Phi_{32} * \Phi_{21}) * G_{11 \setminus \{3\}} * \Phi_{13})^{*-1}$$

entries: a *FINITE* number of operations

*-product: integration !

kernel: K

*-inverse: Neumann series (analytical), Volterra (numerical) 28

A study case: RF artefacts in MRI

see: Balac, Chupin, *Mag. Res. Imaging*, 2008

$$\frac{d}{dt} M(t) = \begin{pmatrix} -\frac{1}{T_2} & -\omega & -v(t) \\ \omega & -\frac{1}{T_2} & -u(t) \\ v(t) & u(t) & -\frac{1}{T_1} \end{pmatrix} M(t) + \begin{pmatrix} 0 \\ 0 \\ \frac{1}{T_1} M_0 \end{pmatrix}$$

$$\left. \begin{array}{l} u(t) = \gamma (\sin(\omega_r t) B_y(t) - \cos(\omega_r t) B_x(t)) \\ v(t) = \gamma (\cos(\omega_r t) B_y(t) + \sin(\omega_r t) B_x(t)) \end{array} \right\}$$

$$B_x(t) = (B_1 + u_1) \cos(\omega_r t) + v_1 \sin(\omega_r t)$$

$$B_y(t) = (-B_1 + v_2) \sin(\omega_r t) + u_2 \cos(\omega_r t)$$

u_i, v_i : RF perturbations

NB: if $u_i, v_i = 0$, $u(t) = B_1$, $v(t) = 0$

Φ becomes independent of t ...

A study case: RF artefacts in MRI

$$\frac{d}{dt} M(t) = \begin{pmatrix} -\frac{1}{T_2} & -\omega & -v(t) \\ \omega & -\frac{1}{T_2} & -u(t) \\ v(t) & u(t) & -\frac{1}{T_1} \end{pmatrix} M(t) + \begin{pmatrix} 0 \\ 0 \\ \frac{1}{T_1} M_0 \end{pmatrix}$$

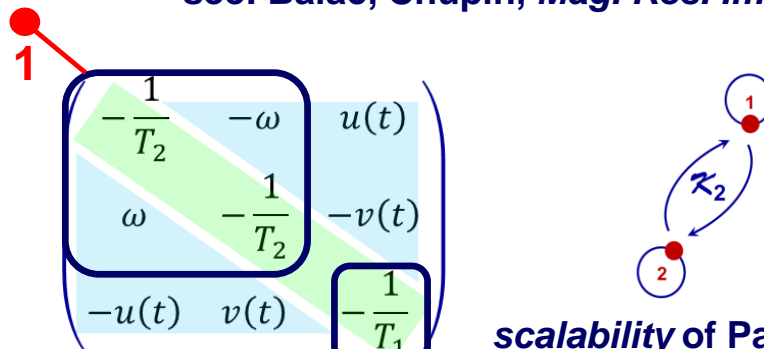
$$\left. \begin{array}{l} u(t) = \gamma (\sin(\omega_r t) B_y(t) - \cos(\omega_r t) B_x(t)) \\ v(t) = \gamma (\cos(\omega_r t) B_y(t) + \sin(\omega_r t) B_x(t)) \end{array} \right\}$$

$$B_x(t) = (B_1 + u_1) \cos(\omega_r t) + v_1 \sin(\omega_r t)$$

$$B_y(t) = (-B_1 + v_2) \sin(\omega_r t) + u_2 \cos(\omega_r t)$$

u_i, v_i : RF perturbations

see: Balac, Chupin, *Mag. Res. Imaging*, 2008



scalability of Path-Sum

$$G_{33} = (1_* - K_{33})^{*-1}$$

$$K_{33} = -\frac{1}{T_1} + (v(t') - u(t')) * \left(\text{Id} \delta(t' - t) + e^{\mathbf{M}(t' - t)} \right) * \begin{pmatrix} -v(t') \\ -u(t') \end{pmatrix}$$

• exact expression of $K_{33} = \sum_0^{10} c_j q_j(t', t)$

$$K_{33} = c_0 + c_1 \cos(2\omega_r t') + c_2 \sin(2\omega_r t') + e^{-\frac{1}{T_2}(t' - t)} \left(c_3 \sin(\omega(t' - t)) + c_4 \cos(\omega(t' - t)) \right)$$

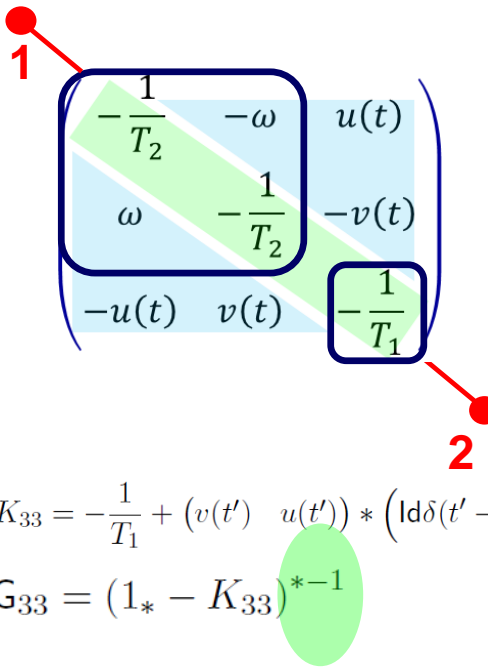
walks avoiding

1

$$\begin{aligned} &+ c_5 \sin((\omega - 2\omega_r)(t' - t)) + c_6 \cos((\omega - 2\omega_r)(t' - t)) \\ &+ c_7 \sin(-2\omega_r t' + \omega(t' - t)) + c_8 \sin(2\omega_r t + \omega(t' - t)) \\ &+ c_9 \cos(2\omega_r t' - \omega(t' - t)) + c_{10} \cos(2\omega_r t + \omega(t' - t)) \end{aligned}$$

resonance at $2\omega_r$

A study case: RF artefacts in MRI



- exact expression of $(1_* - K_{33})^{*-1} = \sum_{n=0}^{\infty} K_{33}^n$

- analytical, unconditionally convergent
Neumann series

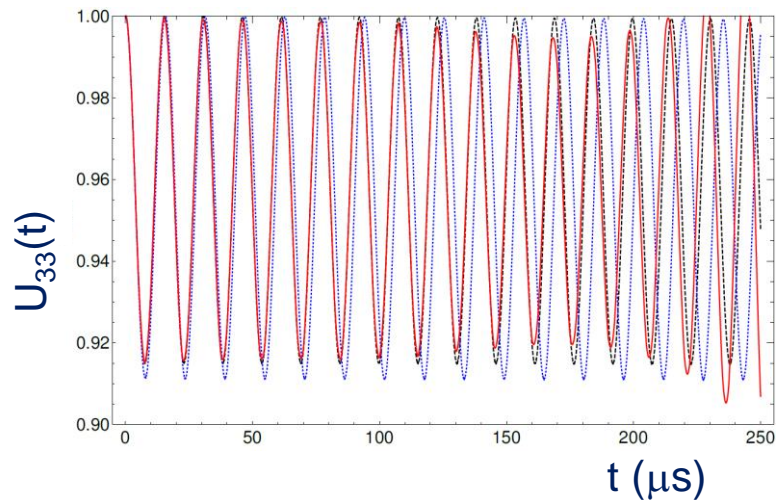
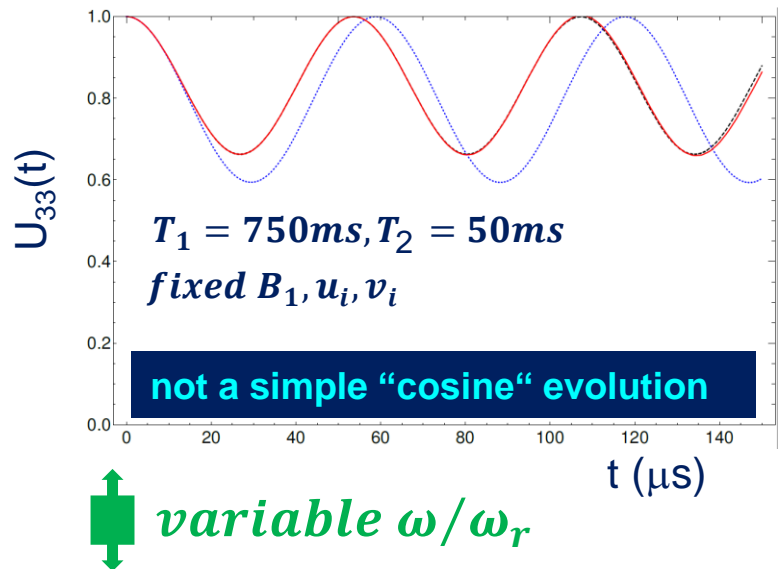
- here: exact forms of the solutions



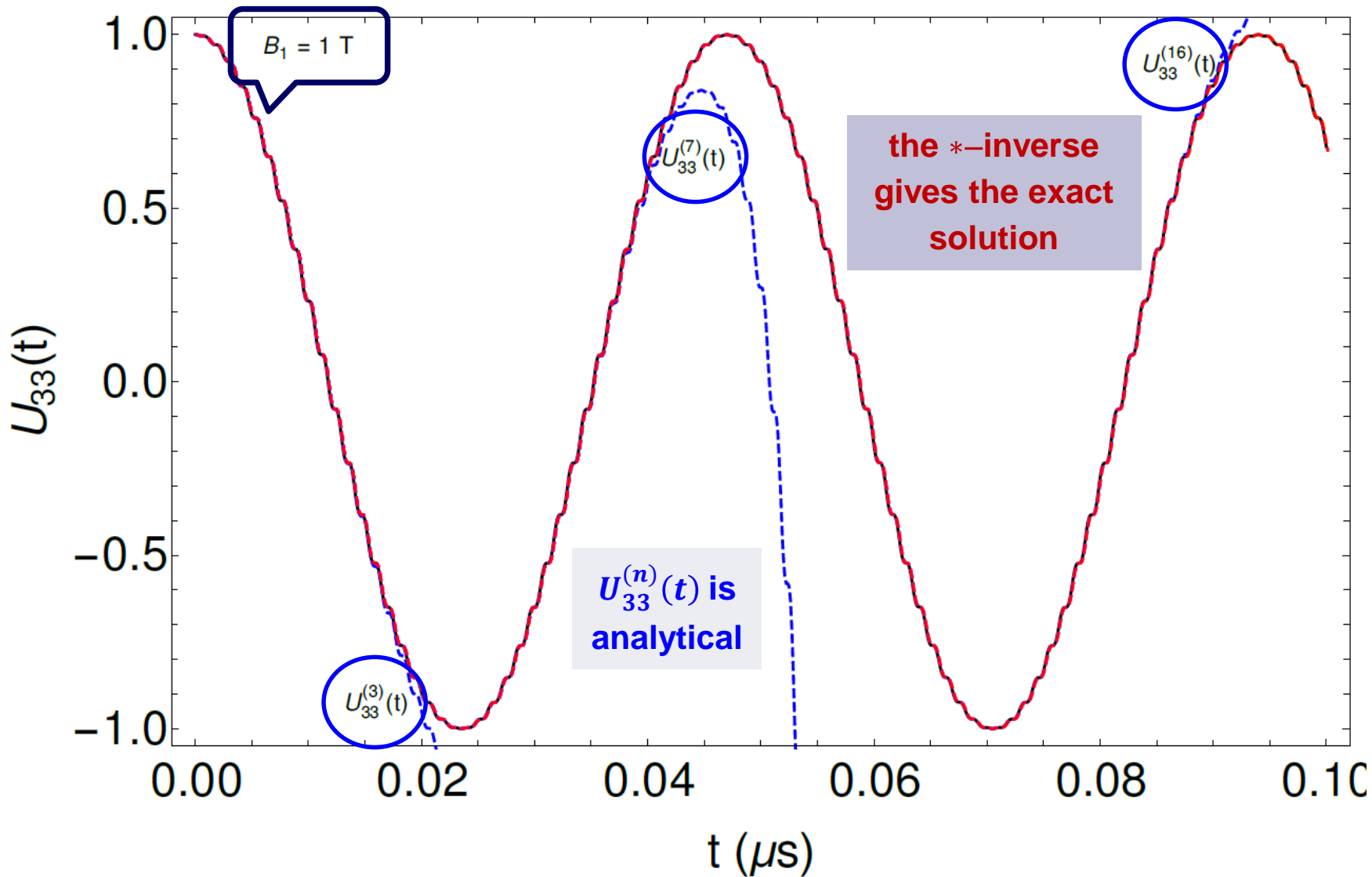
$$U_{33} = C_0(t) + \sum_{k=1}^{\infty} S_{2k\omega_r}(t) \sin(2k\omega_r t) + C_{2k\omega_r}(t) \cos(2k\omega_r t)$$

$$+ \sum_{k=0}^{\infty} S_{\omega \pm 2k\omega_r}(t) \sin((\omega \pm 2k\omega_r)t) + C_{\omega \pm 2k\omega_r}(t) \cos((\omega \pm 2k\omega_r)t)$$

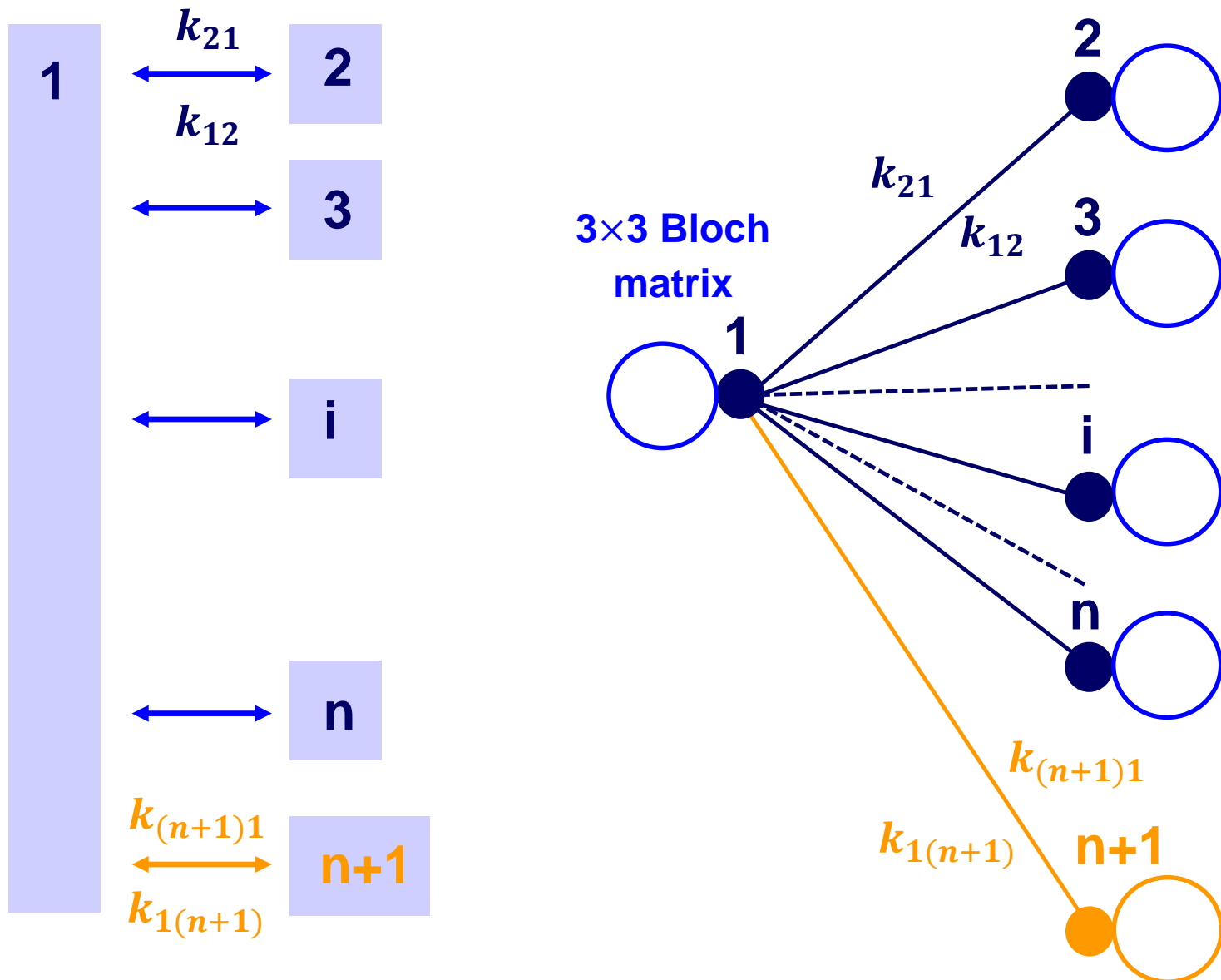
see: Balac, Chupin, *Mag. Res. Imaging*, 2008



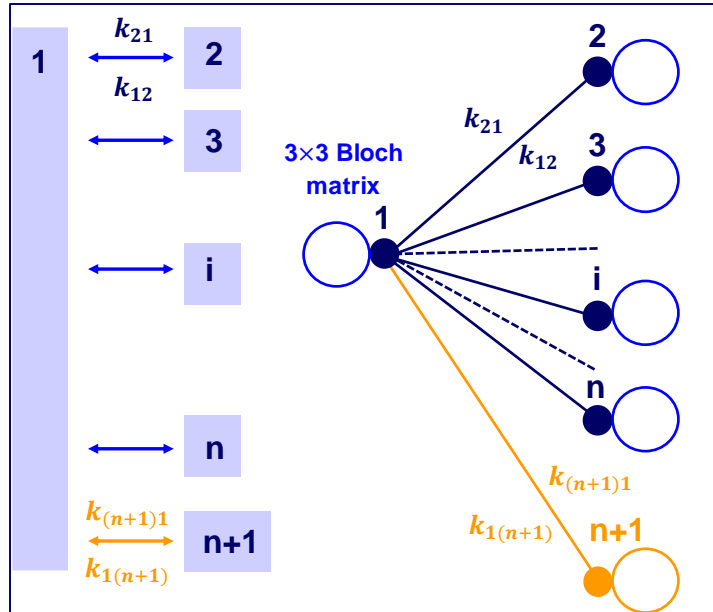
Bloch equations: RF artefacts in MRI



Scale invariance: chemical exchange with n , $(n+1)$ pools



Scale invariance: chemical exchange with n pools (PARTITIONS)



$$K_{ii} \sim \textcircled{i} + k_{i1} * [\text{---}]^{*-1} * k_{1i}$$

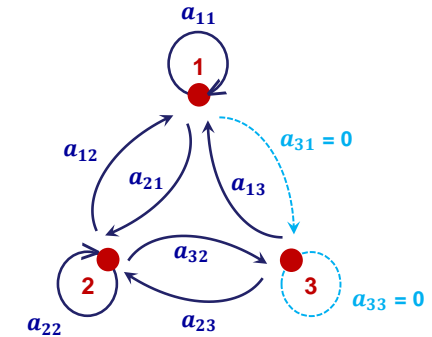
3x3 Bloch matrix

- ▶ the number of terms in K_{ii} is proportional to n
 - ▶ the expression of K_{ii} is always valid (time independent or not)
 - ▶
- $-k_{1(n+1)} * [1_* - \textcircled{n+1}]^{*-1} * k_{(n+1)1}$
is proportional ($k_{1(n+1)} k_{(n+1)1}$) to the integral over time of the propagator of the self-loop

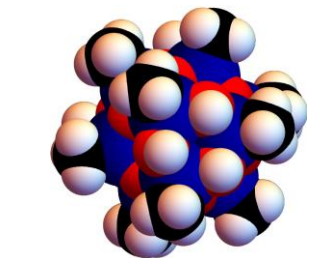
$$\boxed{1_* - k_{12} * [1_* - \textcircled{2}]^{*-1} * k_{21} - \dots - k_{1(n+1)} * [1_* - \textcircled{n+1}]^{*-1} * k_{(n+1)1}}$$

Outline

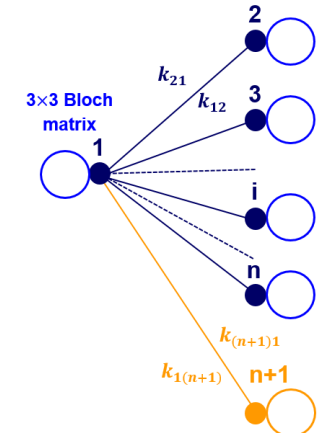
■ Basics of Path-Sum (Giscard)



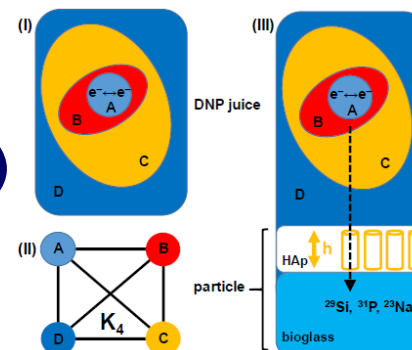
■ Bloch-Siegert effect and spin diffusion in solids

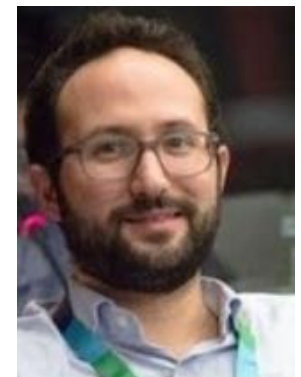
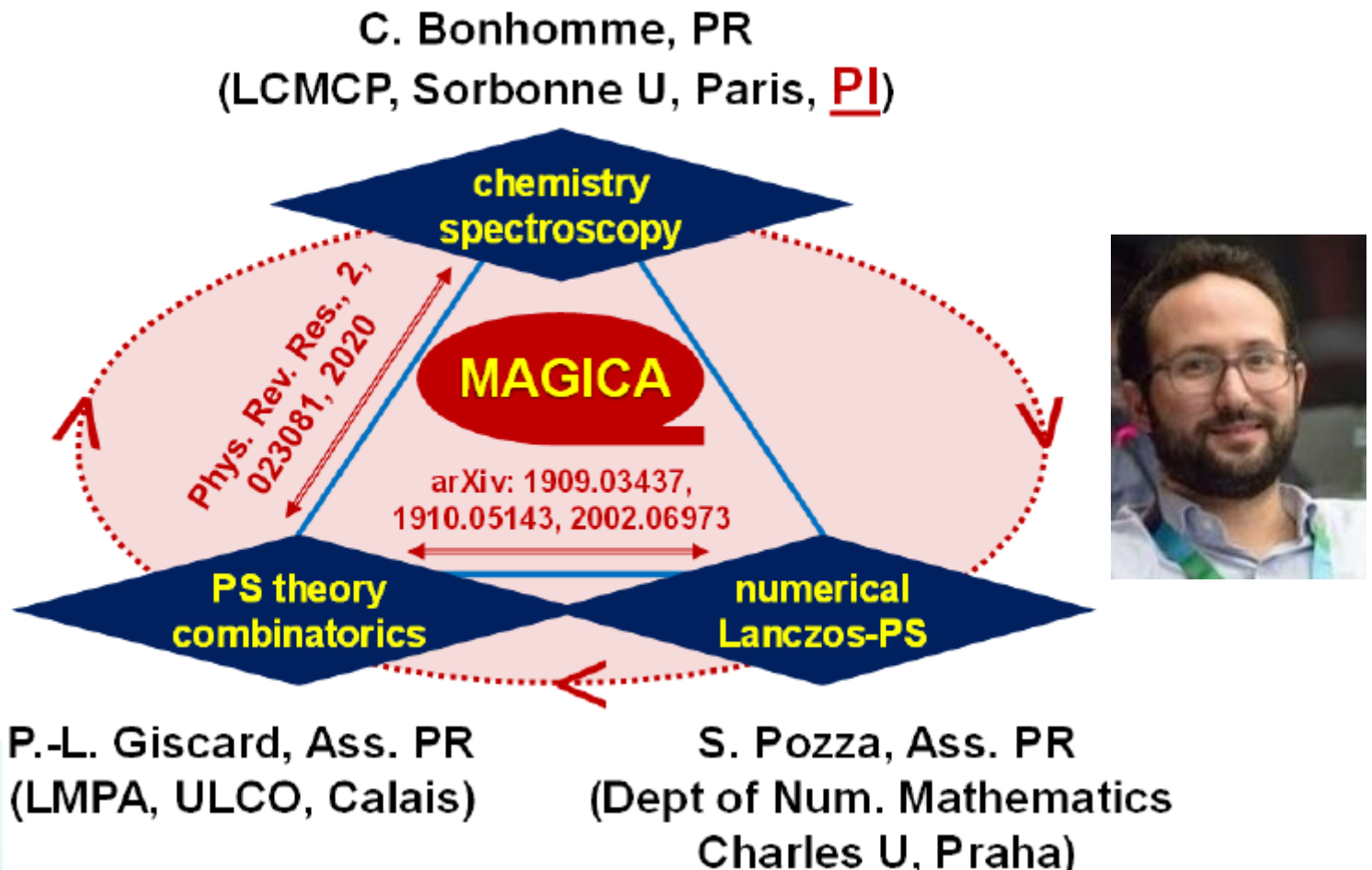


■ Bloch equations in MRI



■ the MAGICA project (2021 →)





WP1. A Path-Sum universal Bloch solver for NMR

✓ Path-Sum applied to Bloch-Torrey, fractional Bloch, Bloch-Torrey equations

$$\frac{\partial m_l(r, t)}{\partial t} = \nabla \cdot (D_l(r) \nabla m_l(r, t)) - i\gamma B(r, t) m_l(r, t) - \frac{1}{T_l} m_l(r, t) - v(r, t) \cdot \nabla m_l(r, t)$$



The introduction to the operator method
for solving differential equations.
First-order DE

YU. N. KOSOVTSOV



3 Operator solutions for first-order non-linear
ODE

First-order differential equation of arbitrary form

$$\frac{du(t)}{dt} = f(t, u(t)) \quad (5)$$

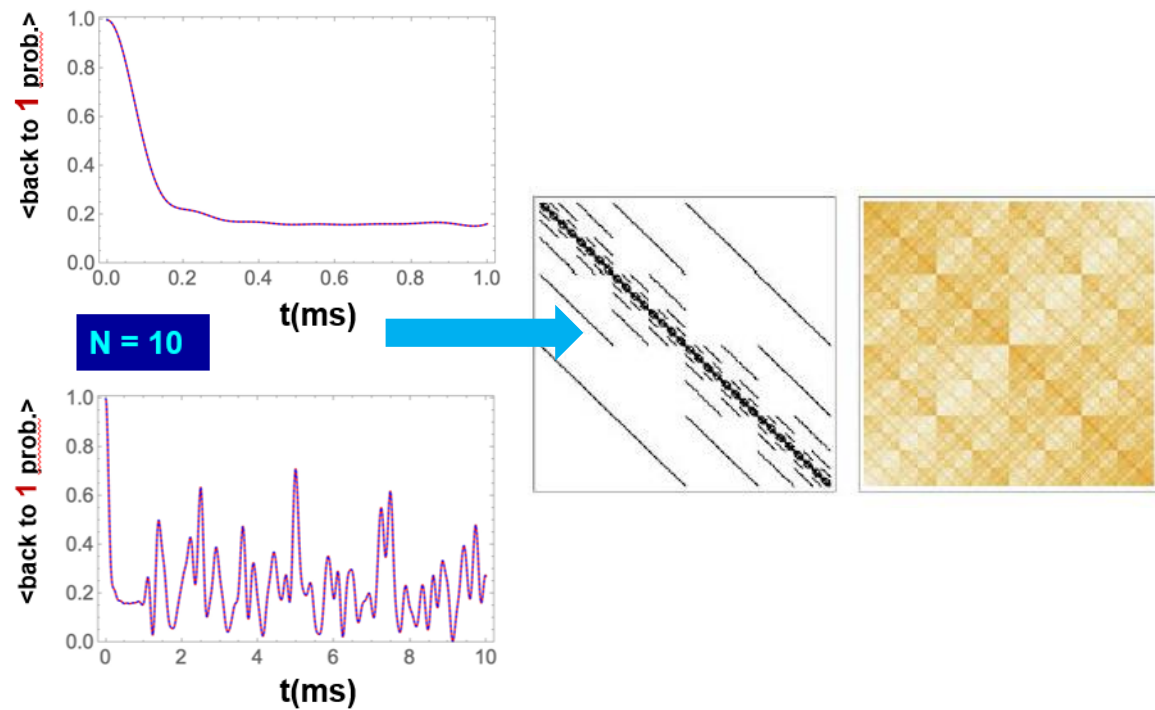
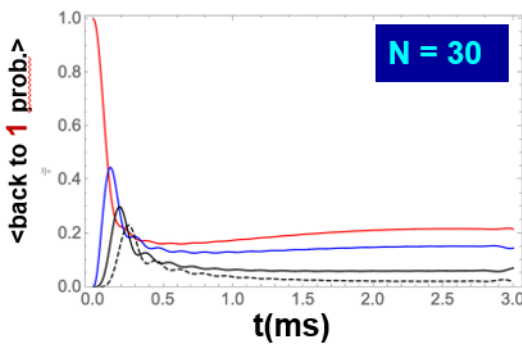
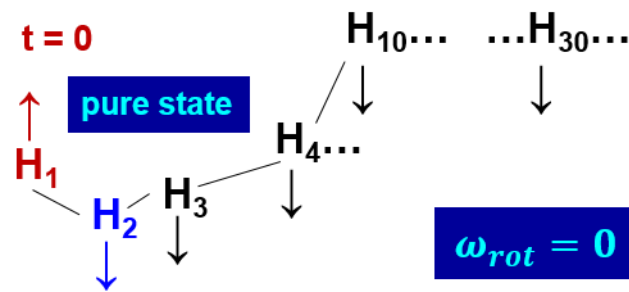
→ diffusion
→ heterogeneous/porous
materials

WP2. Numerical Lanczos Path-Sum and applications: optimal control and ultra-large spin systems

- ✓ Lanczos Path Sum and Optimal Control
- ✓ Path-Sum as a SIMPSON toolbox
- ✓ Infinite chains and DNP

WP2. Numerical Lanczos Path-Sum and applications: optimal control and ultra-large spin systems

- ✓ Lanczos Path Sum and Optimal Control
- ✓ Path-Sum as a SIMPSON toolbox
- ✓ Infinite chains and DNP



WP2. Numerical Lanczos Path-Sum and applications: optimal control and ultra-large spin systems

- ✓ Lanczos Path Sum and Optimal Control
- ✓ Path-Sum as a SIMPSON toolbox
- ✓ Infinite chains and DNP

Pozza, Giscard (2019, 2020)

full $A(t') = \begin{pmatrix} a(t') & b(t') & \dots \\ c(t') & \dots & \dots \\ \dots & \dots & \dots \end{pmatrix}^N$

tridiagonal $T_n(t') = \begin{pmatrix} \alpha_0(t') & 1_* & & & \\ \beta_1(t') & \alpha_1(t') & & & \\ & \vdots & \ddots & & \\ & & \vdots & \ddots & 1_* \\ & & & \beta_{n-1}(t') & \alpha_{n-1}(t') \end{pmatrix}$

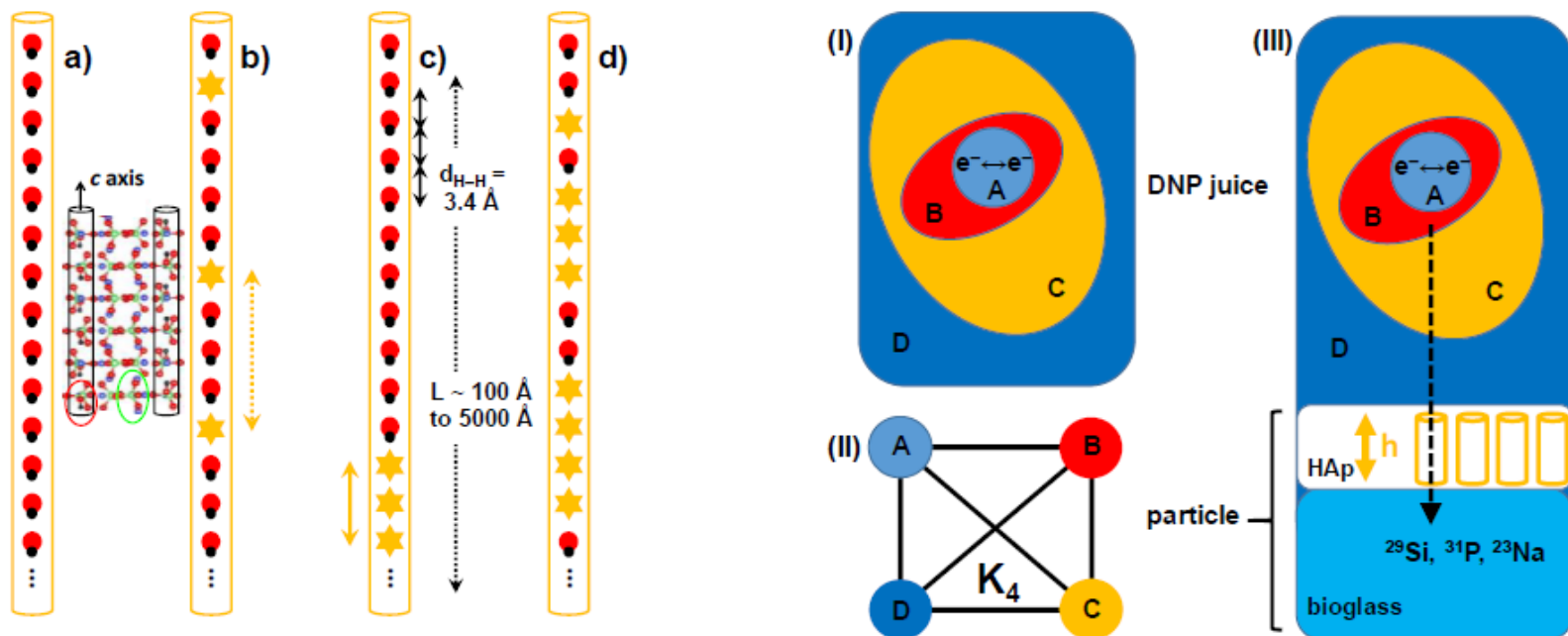
$n \ll N$

*— Lanczos

a very simple continued fraction to handle !

WP3. Experimental NMR and DNP: new insight by Path-Sum

- ✓ Rabi modulated continuous wave spectroscopy and optimal control
- ✓ (T_1, T_2, T_{1r}) "imaging" of pathological calcifications
- ✓ Proton spin diffusion and DNP in substituted hydroxyapatites revisited



Conclusions and acknowledgments

Path-Sum



- ▶ NMR, DNP, ... at ALL levels
- ▶ Machine Learning in NMR
- ▶ and ... FUN!!



MAGICA: **PhD position in Calais + Post-Doctoral position**
available in Calais/Paris

« With application to quantum mechanics, path integrals suffer most grievously from a serious defect. They do not permit a discussion of spin operators or other such operators in a simple and lucid way » (**R.P. Feynman**)

- Path-sum performs a formal **re-summation** of an infinite number of w , i.e. Feynman diagrams !

